nature human behaviour

The development of aperiodic neural activity in the human brain

A list of authors and their affiliations appears at the end of the paper

The neurophysiological mechanisms supporting brain maturation are fundamental to attention and memory capacity across the lifespan. Human brain regions develop at different rates, with many regions developing into the third and fourth decades of life. Here, in this preregistered study (https://osf.io/gsru7), we analysed intracranial electroencephalography recordings from widespread brain regions in a large developmental cohort. Using task-based (that is, attention to to-be-remembered visual stimuli) and task-free (resting-state) data from 101 children and adults (5.93–54.00 years, 63 males; n electrodes = 5,691), we mapped aperiodic (1/f-like) activity, a proxy of neural noise, where steeper slopes indicate less noise and flatter slopes indicate more noise. We reveal that aperiodic slopes flatten with age into young adulthood in both association and sensorimotor cortices, challenging models of early sensorimotor development based on brain structure. In the prefrontal cortex (PFC), attentional state modulated age effects, revealing steeper task-based than task-free slopes in adults and the opposite in children, consistent with the development of cognitive control. Age-related differences in task-based slopes also explained age-related gains in memory performance, linking the development of PFC cognitive control to the development of memory. Last, with additional structural imaging measures, we reveal that age-related differences in grey matter volume are similarly associated with aperiodic slopes in association and sensorimotor cortices. Our findings establish developmental trajectories of aperiodic activity in localized brain regions and illuminate the development of PFC control during adolescence in the development of attention and memory.

Human brain regions develop at different rates, with many regions developing into the third and fourth decades of life, followed by gradual declines in volume throughout adulthood[1–3]. Understanding the complexities of human brain development requires a comprehensive investigation into the intricate interplay between electrophysiological dynamics, brain structure and behaviour across the lifespan. Despite the importance of this endeavour to basic and translational neuroscience, research has been limited by a paucity of methods capable of studying human brain function with high spatial and temporal precision and focused on narrow age ranges. Furthermore, non-oscillatory,

aperiodic activity has yet to be fully characterized from a developmental perspective (cf. refs. 4–7). Consequently, the manifestation of age-related differences in aperiodic activity and their relation to brain structure and cognition remain unknown.

The aperiodic component of the electrophysiological power spectrum, characterized by its spectral slope and offset[8,9], is hypothesized to reflect neural noise[10,11], with a flatter slope and lower offset posited to reflect increased excitatory neuronal population spiking[12,13]. While there are several interpretations of the aperiodic signal, it is probably produced by a variety of biological mechanisms[14–16], including
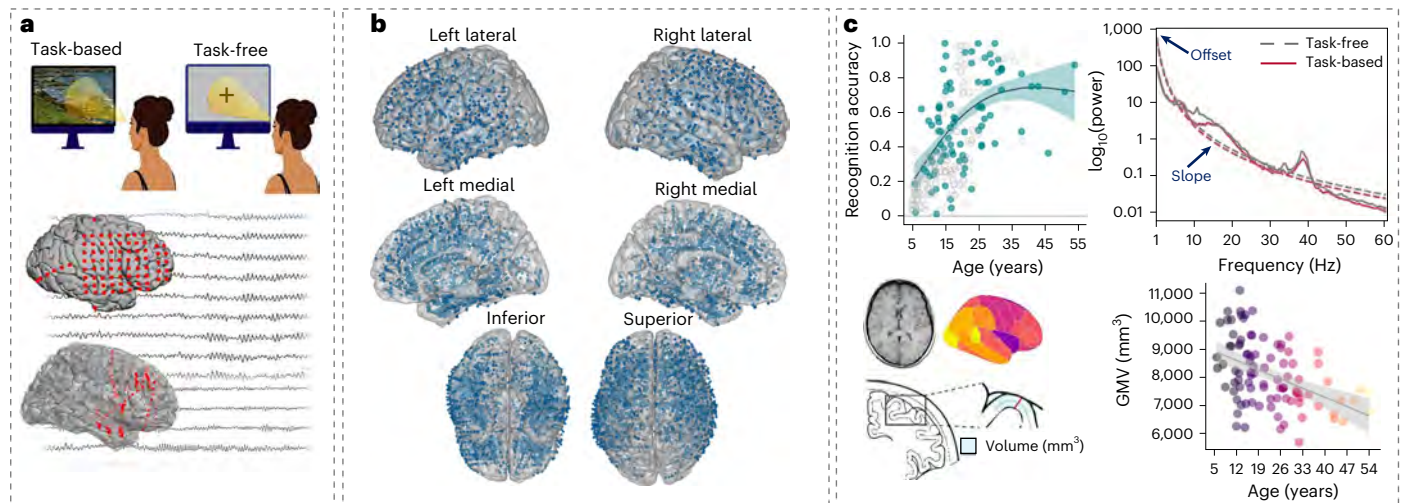
✉ e-mail: zachariah.cross@northwestern.edu

Fig. 1 | Design, channel coverage and key variables. a, Intracranial neurophysiological activity was recorded using ECoG (middle) and sEEG (bottom) during both task-based (top left) and task-free (top right) wake states. **b**, Seizure- and artefact-free intracranial channel placements ($n = 5,691$) across all patients ($n = 101$) in MNI space. **c**, A schematic of key dependent and independent variables. Top left: iEEG patients (teal; $n = 81$) show the expected developmental trajectory of improved memory recognition from ~5 to 30 years of age (one-sided nonlinear regression, $P < 0.001$) and fall in the range of age-matched, healthy controls (grey; $n = 221$). Shading indicates 83% CIs. Top right: schematic PSD plot illustrating the periodic (oscillatory) components over and above the aperiodic ($1/f$-like) component in task-free (dashed) and task-based (solid) conditions. The offset (that is, y intercept) and slope (exponent) make up the aperiodic component when power (y axis) is in log-space. Bottom left: T1 MRI (T1-weighted magnetic resonance image) obtained for each patient, parcellation of cortical regions based on the DKT atlas, and GMV estimation (adapted from ref. 1). Bottom right: age-related differences in global GMV (mm^3) in our cohort, showing the expected developmental trajectory of decreased GMV from ~5 to 54 years of age (one-sided linear regression, $P < 0.001$).

low-pass filtering property of dendrites[17], frequency dependence of current propagation in biological tissues[18], stochastically driven damped oscillators with different relaxation rates[19] and/or the balance between excitation and inhibition (E/I) in neuronal populations[20,21]. From this perspective, this broad range of biological factors probably makes up the aperiodic signal and reflects age-related differences in neural 'noise'.

The balance of optimal levels of neural noise is a fundamental property of healthy brain function[22]. Indeed, optimal levels of neural noise are proposed to safeguard against hypersynchronization, with imbalances in noise implicated in neurodevelopmental disorders, such as schizophrenia and autism[23–25], and generalized learning disabilities[26]. Studies using scalp electroencephalography (EEG) during passive (that is, task-free) states have consistently demonstrated a flattening of the slope and a downward shift in the offset with advancing age throughout adulthood[8,16,27,28]. Such age-related flattening in task-free aperiodic activity predicts declines in memory performance[16] and alterations in stimulus-related neurophysiological responses, such as intertrial alpha phase clustering during visual spatial discrimination in the elderly[29]. By contrast, flatter task-based aperiodic slopes are associated with enhanced memory and learning in healthy young adults[30,31], hinting at a nuanced interplay between aperiodic activity, attentional state and age. Thus, understanding the development of aperiodic activity and its modulation by attentional state, with high spatial precision, is necessary to understand brain development and cognitive function across the lifespan.

So far, developmental studies of aperiodic activity have relied on scalp EEG[4–6,32]. Yet, scalp EEG is limited in spatial resolution and cannot reliably characterize regionally precise neurophysiological activity[33–35]. To overcome these limitations, we analysed rare intracranial EEG (iEEG) data from an exceptionally large developmental cohort of neurosurgical patients aged 5–54 years undergoing invasive monitoring for seizure management. In contrast to non-invasive neuroimaging, iEEG provides both spatially localized information and the high temporal precision needed to examine neurophysiology[36–38] and is thus an invaluable tool for investigating mechanisms of cognitive and brain

maturation[33,39–44]. iEEG provides rich and novel measures of neurophysiology including low-frequency periodic and aperiodic activity, and high-frequency broadband activity reflecting neuronal population activity[45–49]. Thus, iEEG enables unique discoveries of the neurophysiological mechanisms of cognitive and brain maturation in humans.

In this preregistered study (https://osf.io/gsru7), we sought to define regionally precise, brain-wide developmental trajectories of aperiodic activity in task-based and task-free states (Fig. 1a,b). In addition to mapping aperiodic activity across development, we defined the relationship between regionally precise aperiodic activity and cortical structure (Fig. 1c). Measures of regional grey matter volume (GMV) and electrophysiological activity show substantial overlap in relation to cognition, pathology[50,51] and age[52–55], which suggests that they may be jointly explained by shared factors, such as myelination and synaptogenesis. Thus, examining structure–function coupling can provide context to understand novel electrophysiological findings, such as iEEG measures of aperiodic activity by age, based on well-documented age-related variability in regional brain structure[1,2,56]. Based on reports of age-related variability in global scalp EEG-derived aperiodic activity[5,6,32,57,58] and in brain structure demonstrating that sensorimotor regions mature earlier than association regions[2,3,59,60], we hypothesized the following: (a) in association cortices, the aperiodic slope flattens with age into young adulthood; (b) in sensorimotor cortices, the aperiodic slope flattens with age into adolescence; (c) attentional state (task-based versus task-free) modulates age effects observed in (a) and (b); and (d) age-related differences in aperiodic activity are modulated by regional GMV.

We first reveal a gradient in aperiodic activity across the brain, suggesting less neural noise in inferior lateral posterior regions and more neural noise in superior medial frontal regions. We then establish developmental trajectories of aperiodic activity, revealing a flattening of the slope from childhood to young adulthood in both association and sensorimotor cortices, challenging our hypothesis that aperiodic activity stabilizes before young adulthood in sensorimotor cortices. We further reveal how attentional state modulates age effects in select regions including the prefrontal cortex (PFC) and establish predictive

links between task-based aperiodic activity in the PFC and individual memory outcomes. Finally, we uncover novel associations between cortical structure and function, highlighting how aperiodic slopes in both association and sensorimotor cortices are modulated by age-related variability in GMV. Taken together, we offer critical insights into the intricate interplay between aperiodic neural activity, cortical structure and behaviour from childhood to middle age and illuminate the development of PFC control during adolescence in the development of attention and memory.

Results

iEEG memory and brain volume measures are generalizable

In total, 101 neurosurgical patients participated (mean age 19.25, range 5.93–54.00 years; 63 males). Patients were selected on the basis of above-chance behavioural performance on two visual memory recognition tasks (mean normalized accuracy 0.54, standard deviation (s.d.) 0.25, range 0.01–1.00; $\beta = 0.54$, s.e.m. 0.02, $P < 0.001$) and/or if there was a task-free recording available. Those with major lesions, prior surgical resections, noted developmental delays or neuropsychological memory test scores <80 were considered ineligible. A nonlinear regression (single spline with two internal knots) of recognition accuracy by age indicated a positive association (first knot: $\beta = 0.90$, s.e.m. 0.16, $P < 0.001$; second knot: $\beta = 0.30$, s.e.m. 0.13, $P = 0.027$; $R^2 = 0.27$; Fig. 1c), indicating that iEEG patients exhibit the expected developmental trajectory of improved memory from age 5 to 30 years, consistent with age-matched, healthy controls[33,40,61]. Analysis of global GMV by age indicated a negative association ($\beta = -46.56$, s.e.m. 9.36, $P < 0.001$, $R^2 = .20$; Fig. 1c), indicating that, with every 1-year increase in age, there is a 47-mm^3 reduction in GMV. This further demonstrates that iEEG patients show the expected developmental trajectory of decreased GMV from age 5 to 54 years, consistent with well-documented decreases in GMV from childhood through adulthood in healthy individuals[1,2,56,62]. These demonstrations provide converging evidence that the results of our iEEG analyses generalize to healthy populations[41,63].

Aperiodic activity differs by brain region

Before testing hypotheses, we first characterized regional differences in aperiodic activity by implementing linear mixed-effects models, regressing region onto the aperiodic slope while regressing out attentional state (task-based, task-free) and age, treating participants and nested channels as random intercepts[41]. Regions of interest (ROIs) were defined on the basis of the Desikan–Killiany–Tourville (DKT) atlas[64]. The goodness of fit (that is, R^2) between task-based (mean (M) = 0.93, s.d. 0.05) and task-free (M = 0.94, s.d. 0.05) conditions indicated good fits (see Supplementary Fig. 15 for the distribution of model fits between conditions). We revealed a gradient of steeper slopes in inferior lateral posterior regions to flatter slopes in superior medial frontal regions ($\chi^2(19) = 1,038.30$, $P < 0.001$; Fig. 2a). These results extend previous reports of a posterior-to-anterior gradient in task-free neural noise based on functional magnetic resonance imaging (fMRI; that is, Hurst exponent[65]) and the magnetoencephalography aperiodic component[66]. Our data demonstrate that aperiodic activity varies between localized brain regions to a higher degree than previously reported.

Second, to characterize relationships between regional GMV and aperiodic activity (that is, structure–function coupling), we correlated regional aperiodic slopes with regional GMV. We revealed regionally specific relationships between aperiodic activity and GMV (Fig. 2b–d). We observed a significant positive correlation with slope and GMV in the rostral middle frontal gyrus (rMFG; $r = 0.27$, $P_{adj} = 0.038$, 95% confidence interval (CI 0.04 to 0.48), and a significant negative correlation in the inferior temporal cortex ($r = -0.22$, $P_{adj} = 0.038$, 95% CI −0.40 to −0.01). These results reveal opposing structure–function coupling between localized regions and indicate that there is not a one-to-one mapping between GMV and aperiodic activity.

Aperiodic activity stabilizes in young adulthood

Having demonstrated that aperiodic activity differs by brain region, we sought to establish developmental trajectories of aperiodic activity between association and sensorimotor cortices. We first examined hypothesis (a), that in association cortices, the aperiodic slope flattens with age into young adulthood, and hypothesis (b), that in sensorimotor cortices, the aperiodic slope flattens with age into adolescence (see Supplementary Table 1 for a summary of association and sensorimotor regions). We implemented nonlinear mixed-effects regressions, modelling aperiodic activity as a function of age (fit with one spline; two knots) and cortex type (association, sensorimotor; Supplementary Table 1), treating participant and DKT region as random effects on the intercept, and channel nested under participant. We revealed a significant age × cortex type interaction ($\beta = 0.22$ (95% CI 0.14 to 0.30), s.e.m. 0.04, $P < 0.001$; see Supplementary Fig. 1 for model diagnostics), demonstrating that the slope flattens with age into young adulthood, with the greatest flattening difference in sensorimotor compared with association cortices at 30 years of age ($\beta = -0.18$, s.e.m. 0.08, $P = 0.021$; Fig. 3). These results support our hypothesis that the aperiodic slope flattens with age into young adulthood in association cortices. These results are contrary to our hypothesis that aperiodic activity stabilizes with age into adolescence in sensorimotor cortices; however, the difference in flattening suggests dissociable trajectories between association and sensorimotor cortices.

Aperiodic activity differs by age and attentional state

We next sought to establish developmental trajectories of aperiodic activity within localized brain regions and test hypothesis (c), that age effects would differ between attentional states. To identify regional age effects in aperiodic activity and whether they differ by attentional state, we implemented separate linear mixed-effects models for each ROI. Our strategy for each analysis was to fit a model to the aperiodic slope and regress the estimates onto age (in years), attentional state (task-based, task-free) and the interaction of age and attentional state. All models were fit with by-participant and by-task random intercepts, with channel nested under participant (see Supplementary Figs. 2 and 3 for model diagnostics).

We revealed significant age × attentional state interactions in the caudal middle frontal gyrus (cMFG; $\beta = -0.003$ (95% CI −0.006 to −0.002), s.e.m. 0.001, $P_{adj} = 0.007$) and rMFG ($\beta = -0.004$ (95% CI −0.008 to −0.002), s.e.m. 0.001, $P_{adj} = 0.045$). In both cMFG and rMFG, task-free slopes are steeper than task-based slopes in children, and the opposite is observed in adults; the direction of differences reverses around age 18–20 years (Fig. 4). If flatter slopes imply greater neural noise, and PFC activity reflects cognitive control, then these results are consistent with increased cognitive control during task engagement in adolescence[60,67–69] and mirror the development of domain-general cognitive control[70]. These results also support our hypothesis that attentional state modulates age-related flattening of the aperiodic slope. For visualizations of the main effects of age and condition on the aperiodic slope, see Supplementary Figs. 4 and 5, respectively.

Task-based slopes in association cortices predict memory

Having demonstrated that memory performance improves with age, with marked variability among adolescents (Fig. 1c), we examined whether age interacts with regionally specific task-based and task-free aperiodic slopes, respectively, to predict memory performance. For each analysis, we fit a general linear model to recognition accuracy and regressed the estimates onto age (in years) and aperiodic slopes (task-based or task-free), and the interaction of age and slope. For task-based slopes (after accounting for the unique contribution of age) we observed an age × slope interaction in the rMFG ($\beta = 0.02$ (95% CI 0.009 to 0.04), s.e.m. 0.01, $P_{adj} = 0.046$; $R^2 = .40$; Fig. 5). In the rMFG, memory performance increases with age and an age-related flattening of the aperiodic slope. Although overall steeper slopes were observed
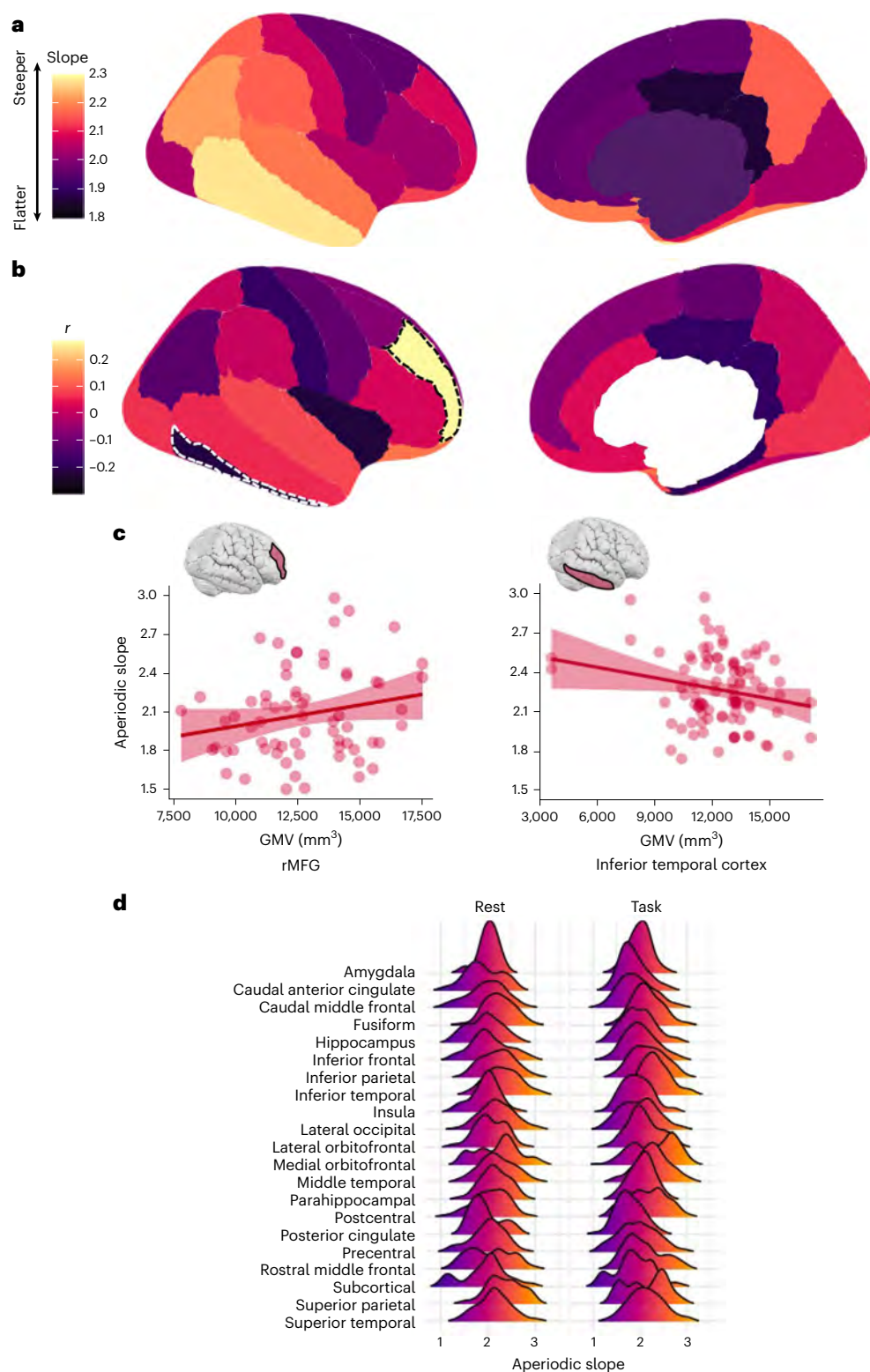
Fig. 2 | Regional differences in the aperiodic slope and correlations with GMV. a, Brain-wide standardized means (predicted marginal means) of regional aperiodic slopes adjusted across attentional state, age and the random effects structures. Warmer colours/higher values indicate steeper slopes. **b**, Brain-wide correlations (one-sided, false discovery rate (FDR)-corrected Spearman correlations) between regional GMV (mm³) and aperiodic slopes. Warmer colours/higher values indicate positive correlations; cooler colours/lower values indicate negative correlations. Note that the area corresponding to subcortical space is white as no analysis of subcortical GMV was performed. Regions with statistically significant correlations ($P < 0.05$) are indicated by dashed borders. **c**, Scatter plots illustrating relationships between GMV (x axis) and aperiodic slopes in regions with statistically significant correlations. Individual data points represent single participant data averaged across channels for each representative ROI. Shading shows the standard error. **d**, A ridgeline plot illustrating the distribution of aperiodic slopes (x axis; higher values denote a steeper slope) by region (y axis) and condition (left: task-free; right: task-based).
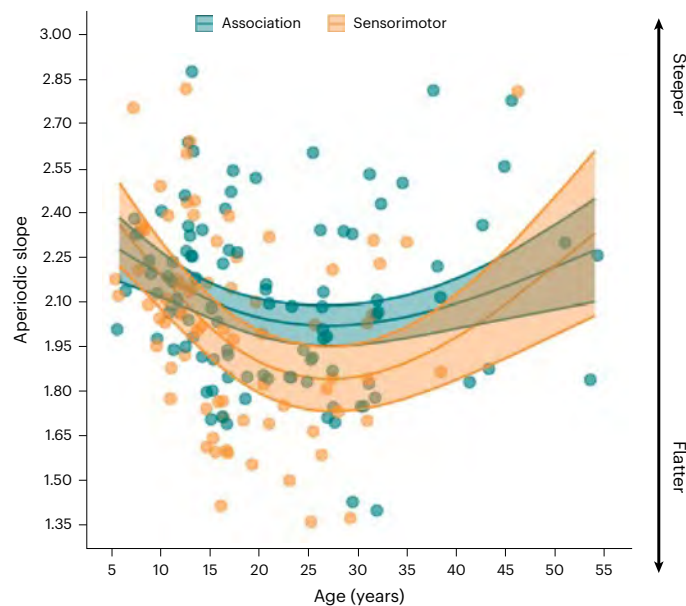
Fig. 3 | Age-related differences in aperiodic slopes between association and sensorimotor cortices. Modelled effects for differences in the aperiodic slope (*y* axis; higher values denote a steeper slope) by age (*x* axis). Association cortices are presented in teal and sensorimotor cortices in orange. Shading indicates 83% CIs. Individual data points represent slope values per participant averaged over channels.

in children, relatively flatter slopes in children and adolescents were associated with relatively superior memory. There were no other significant main effects of the task-free slope or interactions between the task-free slope and age on memory performance (all $P > 0.05$). For visualizations of model diagnostics, see Supplementary Figs. 6 and 7, and for main effects of task-based and task-free slopes on memory, see Supplementary Figs. 8 and 9, respectively.

Taken together, our results elucidate how age-dependent effects on aperiodic slopes in PFC predict individual memory performance. These effects were evident exclusively during task-based states, thus linking aperiodic activity during attention to to-be-remembered visual information to an individual's memory for that information. From this perspective, the aperiodic slope may serve as a key marker of typical and atypical memory development.

Brain structure and age interact to predict aperiodic activity
Thus far, we have established that aperiodic slopes in PFC differ by age and attentional state and predict age-related variability in memory outcomes, whereas slopes in sensorimotor regions do not differ by attentional state or predict age-related variability in memory outcomes. Last, we focus on structure–function relationships. Before testing hypothesis (d), that age-related differences in aperiodic activity are modulated by regional GMV, we sought to replicate previous reports of age-related reductions in regional GMV[1,2,56]. Having demonstrated that global GMV decreases with age in our cohort (Fig. 1c), we examined GMV by ROI. We implemented a linear mixed-effects model, regressing region and age onto GMV, treating participants as random intercepts. Our model confirmed a significant main effect of region ($\chi^2(19) = 11,081.98, P < 0.001$) and revealed an age × region interaction ($\chi^2(19) = 92.05, P < 0.001$; Fig. 6). GMV is reduced with age in lateral orbitofrontal cortex ($r = -0.61, P < 0.001$, 95% CI -0.77 to -0.35), medial orbitofrontal cortex ($r = -0.60, P = 0.001$, 95% CI -0.81 to -0.27), rMFG ($r = -0.38, P = 0.007$, 95% CI -0.61 to -0.11), cMFG ($r = -0.42, P < 0.001$, 95% CI -0.60 to -0.20), inferior frontal gyrus ($r = -0.35, P = 0.010$, 95% CI -0.57 to -0.09), superior temporal cortex ($r = -0.40, P = 0.001$, 95% CI -0.59 to -016), middle temporal cortex ($r = -0.33, P = 0.005$, 95% CI

-0.52 to -0.09), posterior cingulate cortex (PCC; $r = -0.36, P = 0.038$, 95% CI -0.62 to -0.02) and inferior parietal cortex ($r = -0.54, P < 0.001$, 95% CI -0.70 to -0.33). These results replicate previous reports of age-related reductions in GMV in association cortices starting in childhood[1,2,56].

To test whether age-related differences in aperiodic activity are modulated by regional GMV, we fit mixed-effects models to task-based slopes and regressed these estimates onto age (in years), GMV and the interaction between age and GMV. All models were fit with by-participant and by-task random intercepts, with channel nested under participant. We revealed age × GMV interactions on task-based aperiodic slopes in the PCC ($\beta = -4.83 \times 10^{-5}$ (95% CI 7.58×10^{-5} to 2.05×10^{-5}), s.e.m. 1.43×10^{-5}, $P_{adj} = 0.040$) and postcentral gyrus ($\beta = -1.08 \times 10^{-5}$ (95% CI -1.79×10^{-5} to -3.80×10^{-6}), s.e.m. 3.57×10^{-6}, $P_{adj} = 0.040$; Fig. 7). In both association and sensorimotor regions (Table 1), while there was no relationship between task-based slopes and GMV in children, flatter slopes were linked with higher GMV in adults. For visualizations of the main effects of age and GMV on aperiodic slopes, see Supplementary Figs. 10 and 13, and for model diagnostics, see Supplementary Figs. 11 and 12, respectively.

Discussion
We mapped aperiodic activity—a marker of neural noise—from childhood to late middle adulthood. Our findings demonstrate: (1) a gradient of slopes from inferior lateral to superior medial regions, suggesting reduced neural noise in inferior lateral temporal regions and increased neural noise in superior medial frontal regions (Fig. 2); (2) a U-shaped relationship in slopes by age, suggesting increased neural noise into young adulthood followed by reduced neural noise into middle adulthood (Fig. 3); (3) a flattening of PFC slopes by age, with more pronounced flattening in task-free states, suggesting that age-related increases in neural noise are task dependent (Fig. 4); (4) PFC-derived aperiodic slopes during task-based states predict age-related variability in memory (Fig. 5); and (5) lower GMV is associated with steeper slopes across age in association and sensorimotor cortices (Fig. 7). In sum, these findings reveal regional and attentional differences in neural noise from early childhood to late middle adulthood and establish the balance of neural noise in PFC as a mechanism of memory development (for a schematic summary of the main results, see Fig. 8).

Aperiodic activity stabilizes during adulthood
The spatiotemporal patterning of cortical maturation progresses from sensorimotor to higher-order association cortices, characterized by heightened plasticity in late-maturing association regions, potentially influencing higher-order cognition in adulthood[60]. Based on these observations, we hypothesized that aperiodic activity would follow similar developmental trajectories, such that it would stabilize during adolescence in sensorimotor cortices and during young adulthood in association cortices. Indeed, recent work emphasizes that, while sensorimotor regions exhibit a more localized and intrinsic activation pattern, indicative of a more segregated and stable E/I balance, association regions show more integrated and interconnected activity, with a greater reliance on recurrent feedback loops, reflecting a more dynamic and finely tuned E/I balance that develops later in life[71]. Consistent with our hypothesis, we revealed that the aperiodic slope flattens from childhood to young adulthood in association cortices. However, contrary to dominant models of brain development based on structural measures[2,3,60], we found that aperiodic activity in sensorimotor cortices does not stabilize until young adulthood. We further revealed that the magnitude of flattening is greater in sensorimotor than association cortices during adolescence and young adulthood, pointing to a developmental dissociation. Our findings establish that the development of aperiodic activity in sensorimotor regions does not mirror the development of cortical structure and suggest that
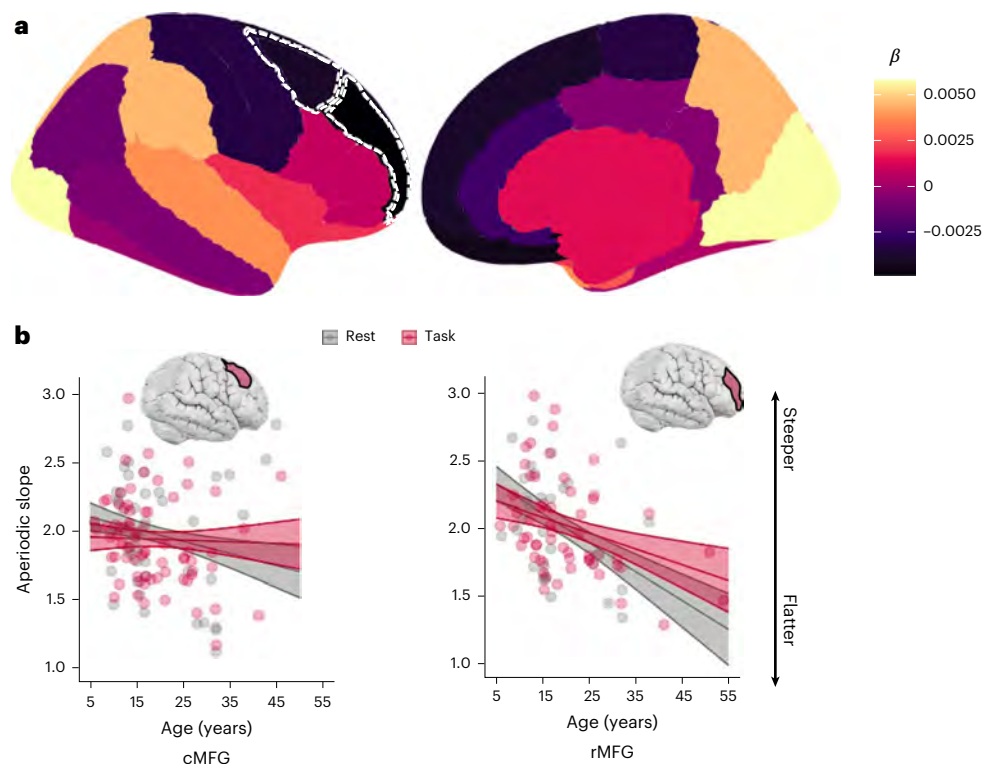
Fig. 4 | Regions with a significant interaction between age and attentional state on aperiodic activity. a, Brain-wide age and condition interactions on regional aperiodic slopes. Regions with statistically significant interactions between age and attentional state (FDR <0.05) are indicated by dashed borders. **b**, Scatter plots illustrating interactions between age (x axis; in years) and attentional state (red, task-based; grey, task-free) on the aperiodic slope (y axis; higher values denote a steeper slope) in regions with statistically significant interactions. Individual data points represent single participant data averaged across channels for each representative ROI. Shading indicates 83% CIs.

developmental differences in neural noise in sensorimotor regions follows a protracted trajectory into adulthood.

Attention modulates aperiodic activity by age in PFC

Scalp-EEG studies have consistently demonstrated an age-related flattening of the aperiodic slope, often with a frontal-central distribution[4,6,27,58,72–74]. To our knowledge, only one iEEG study has examined age-related variability in aperiodic slopes, demonstrating an age-related flattening of task-based slopes in the visual cortex of 15 individuals aged 15–53 years[16]. Little is known regarding regional differences in the slope. We found that subregions of PFC, namely caudal and rostral MFG, exhibit a flattening of the aperiodic slope across age. We further reveal that the age-related flattening of the slope is modulated by attentional state, with less pronounced flattening for task-based relative to task-free states. This finding can be interpreted in the context of PFC control: a central role of the PFC is to exert cognitive control in the service of behaviour, partially by modulating activity in regions further upstream, such as the visual cortex and medial temporal lobe (MTL)[75–77]. The difference between task states also emerges at roughly 18–20 years of age, revealing the aperiodic slope as a potential marker of the development of cognitive control in adolescence, and mirroring the development of domain-general cognitive control[70]. Functionally, steeper task-based slopes, suggesting reduced neural noise, have been proposed to reflect the maintenance of top-down predictions[30,78] and support information integration[72,79]. By contrast, flatter slopes have been associated with slower processing speed[74], and poorer visual working[8] and visuomotor[80] memory, although these studies analysed task-free slopes. Our findings suggest that the PFC gains flexibility in control with age, exerting increased control during the processing of task-relevant information.

Task-based aperiodic activity in PFC predicts memory

Do age-related differences in aperiodic activity predict age-related differences in memory? Prior work on aperiodic activity has reported mixed findings in relating the slope and offset to various aspects of cognition. Steeper task-free slopes have been associated with faster reaction times in young adults and improved recognition accuracy during initial learning[80]. However, in the same study, flatter slopes and higher offsets were associated with improved recognition with increasing task exposure. In a similar study with young adults, flatter task-free slopes and higher offsets were associated with improved decision-making performance[81]. Of the studies examining task-based aperiodic activity, flatter slopes have been associated with improved learning of an artificial language in young adults aged 18–40 years[30], but lower working memory performance with age from 15 to 53 years[16]. Critically, past work has focused on either task-based or task-free aperiodic activity and cognition without accounting for differences between task states, and it is unknown how task-based differences in localized brain regions relate to behaviour by age.

Here, we overcame this limitation by mapping task-based and task-free aperiodic slopes by age to behaviour on a region-by-region basis. We revealed an interaction between aperiodic slopes and age on memory in the MFG. In the MFG—a region core to executive functions and cognitive control and that undergoes protracted development[82,83]— children with steeper slopes exhibited worse memory performance. This finding suggests that too little noise[8,16] in the MFG during childhood may hinder attentional control. Indeed, children diagnosed with attention deficit hyperactivity disorder who are medication-naive exhibit steeper slopes than their typically developing counterparts[84], as do individuals with schizophrenia[85,86], suggesting that even greater reductions in neural noise in childhood results in inefficient neural
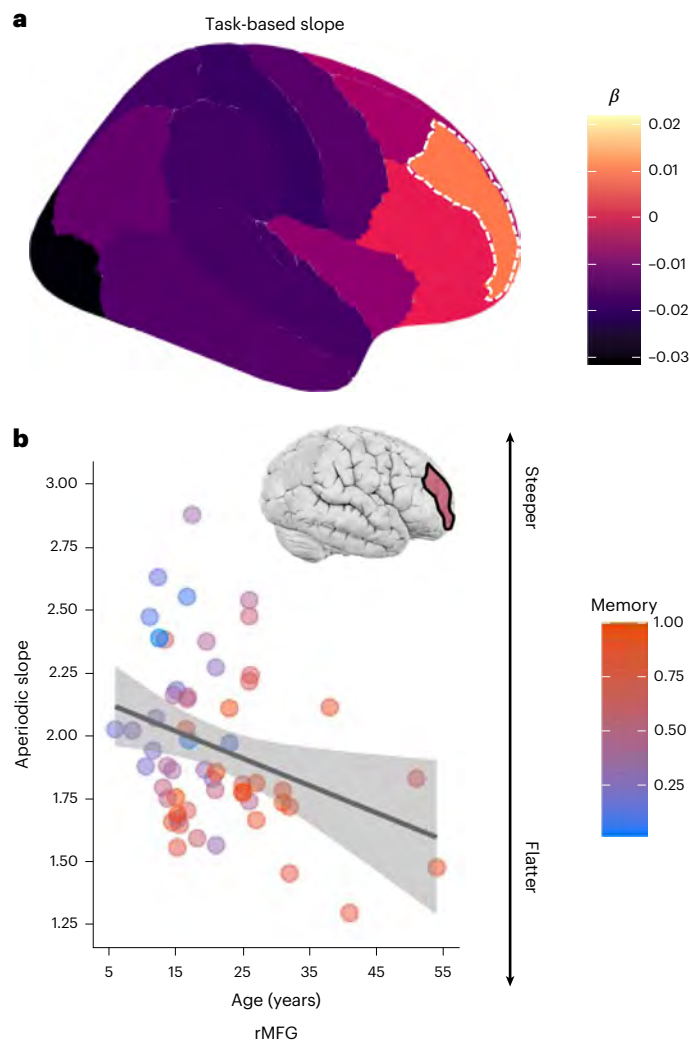
a

Task-based slope

b

Fig. 5 | Task-based aperiodic slopes in the MFG predict age-related differences in memory performance. a, Brain-wide slope and age interactions on memory (one-sided, FDR-corrected linear regressions), with the rMFG demonstrating statistically significant interactions between the task-based slopes and age (*P* < 0.05) on memory performance, with this indicated by dashed borders. **b**, A scatter plot illustrating interactions between task-based rMFG slopes (*y* axis; higher values denote a steeper slope) and age (*x* axis; in years) on memory (*z* scale; warmer colours denote higher memory recognition accuracy). Individual data points represent single participant data averaged across channels for each representative ROI. Shading shows the standard error.

communication and disrupted coordination, manifesting in poorer memory outcomes.

As individuals age, structural and functional changes in MFG (that is, synaptic pruning and changes in neurotransmitter levels (GABAergic interneurons and glutamate)[87]) probably lead to a flattening of aperiodic slopes[88,89]. Flatter slopes have been likened to increased neural noise[16,72,78,90], due to increased levels of aberrant neural firing in the absence of a slower modulatory oscillation[15,16]. We observed that flatter slopes in the MFG during adulthood were less related to memory outcomes than in children, probably due to the emergence of compensatory neural recruitment and altered cognitive strategies[91–93].

Interestingly, we did not observe significant relationships between task-free slopes and memory performance. This apparent discrepancy with past findings can probably be explained by differences in experimental task designs and interregional source mixing inherent to scalp-EEG, where signals from multiple cortical areas are mixed owing to volume conduction[34,35]. Scalp EEG, with its relatively low spatial

resolution, could mask region-specific relationships between aperiodic slopes and behaviour, explaining discrepancies with previous findings. Although source localization techniques can help to mitigate these issues, they are limited in resolving precise cortical sources[94,95]. Furthermore, previous work has focused on mapping intrinsic, task-free aperiodic activity onto trait-like measures of cognition (for example, processing speed and verbal ability[96–98]) or tasks that do not measure episodic or working memory[80,81,90]. Our findings demonstrate that aperiodic activity during the encoding of visual stimuli predicts recognition of those stimuli, a direct relationship that did not survive on a region-by-region basis with intrinsic (that is, task-free) activity.

Aperiodic activity relates to age-related variability in GMV

Finally, having established that aperiodic activity differs by age and attentional state and that task-based aperiodic activity predicts memory outcomes, we mapped task-based aperiodic activity onto GMV across age. We reveal that, in the PCC, aperiodic slopes are not dependent on GMV during childhood. However, as individuals age, the relationship between GMV and aperiodic slopes becomes pronounced. Specifically, individuals who maintain higher GMV in the PCC exhibit a flattening of aperiodic slopes over time. By contrast, those with lower GMV in the PCC during development show stable, steep aperiodic slopes, meaning that their slopes do not differ by age and remain relatively steep across development.

Mechanistically, this pattern may reflect differential cortical maturation and the influence of GMV on neural network stability. In individuals with higher GMV, the gradual stabilization of synaptic networks may facilitate a more balanced cortical state, resulting in flatter aperiodic slopes as they age. In those with lower GMV, however, the lack of such stability may prevent the flattening of the aperiodic slope, leading to a persistently steeper slope despite developmental differences. These findings suggest that early cortical changes in GMV, particularly in the PCC, may be key to understanding the long-term stability of aperiodic neural dynamics and their relationship to cognitive processes such as memory. This should be further elucidated in future work.

Similarly, in the postcentral gyrus (that is, the primary motor cortex), we observed that higher GMV is associated with steeper slopes during childhood and flatter slopes during adulthood. This adds to the finding that sensorimotor cortical development—as indexed by neural noise—stabilizes during young adulthood, challenging models of early sensorimotor development based on cortical structure[1,99]. Future research should further examine relationships between aperiodic activity and brain structure to elucidate the mechanisms by which structure–function development impacts the development of higher-order cognition.

Limitations and future directions

We have revealed regional age-related variations in aperiodic neural activity dependent upon task state. Our findings suggest that brain development may be best understood as a diverse set of regionally independent trajectories, partially indexed by aperiodic activity. However, as iEEG data are cross-sectional, we were unable to follow these putative trajectories through time. A critical next step will be to establish the potential utility of aperiodic activity in elucidating longitudinal changes in regional structure–function relationships[33]. As such, future studies, focusing a priori on the regions we identified (for example, MFG), could capitalize on the spatiotemporal precision and capacity to perform multivisit longitudinal studies with, for example, magnetoencephalography.

While our cohort is representative of typical development and the use of iEEG affords precise spatiotemporal precision, iEEG samples are composed of patients with pharmacoresistant epilepsy, potentially limiting the generalizability of our findings[41]. For this reason, it is important to note that our sample demonstrated typical age-related gains in memory performance and age-related differences
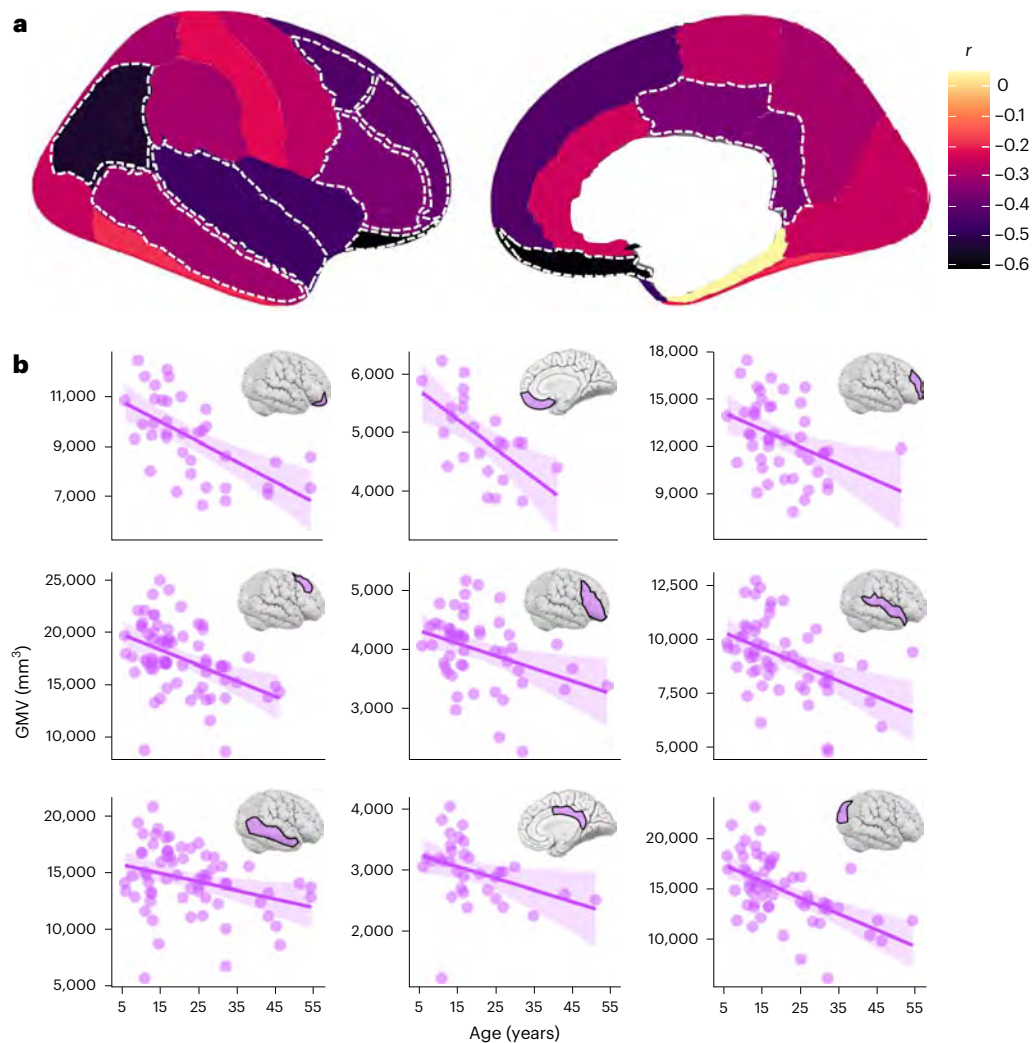
Fig. 6 | Regions with a significant effect of age on GMV. a, Brain-wide correlations (one-sided Pearson *r* correlations) between regional GMV (mm³) and age (in years). Warmer colours/higher values indicate positive correlations and cooler colours/lower values indicate negative correlations. Note that the area corresponding to subcortical space is white as no analysis of subcortical GMV was performed. Regions with statistically significant correlations ($P < 0.05$) are indicated by dashed borders. **b**, Scatter plots illustrating relationships between GMV (*y* axis) and age (*x* axis) in regions with statistically significant correlations. Shaded areas indicate the standard error of the mean.

in global GMV (Fig. 1c), both of which are consistent with healthy cohorts[1,40]. An additional limitation is the relatively lower representation of older individuals within our sample, a common observation in iEEG investigations, and the relatively lower representation of patients with task-free ($n = 65$) compared with task-based ($n = 81$) data. We also acknowledge that there was low sampling of certain brain regions (see Supplementary Tables 2 and 3 for the channel count by region), which may reduce the generalizability of some results. Low sampling reduces statistical power, potentially masking meaningful neural activity or introducing biases in region-specific analyses[40,41]. To address this limitation, we caution readers against overinterpreting non-significant results for regions such as the amygdala, insula and superior parietal cortex. Furthermore, in our analysis, we focused on the frequency range of 1–60 Hz and did not specifically account for the potential influence of a 'knee' in power spectral density (PSD), typically observed around 75 Hz (ref. 100). This knee can result in a shift in PSD scaling behaviour, which may affect the aperiodic slope values if not addressed in the fitting process. Future research should prioritize obtaining more balanced sampling across these regions, possibly by using even larger, more diverse datasets and in using algorithms that account for potential knees in PSD[8]. Nonetheless, the current results

underscore maturation within MFG, and this effect was present across our entire age range of 5–54 years. To obtain larger samples across age, future research may seek to increase sample sizes through multisite collaboration and data sharing[40,41].

We also found no significant age-related difference in aperiodic activity in the hippocampus in relation to attentional state, or in predicting individual memory performance. Given that our study examined memory, these results may be somewhat surprising. However, it is possible that the development of oscillatory (that is, periodic) activity in the hippocampus exhibits effects related to attentional state and memory outcomes, consistent with ample literature on hippocampal theta oscillations[36,44,101,102]. Future research should directly investigate this hypothesis. Lastly, with our task-based versus task-free contrast as a starting point, future research may also aim to examine additional attentional states, such as sleep versus wake states. The aperiodic slope and offset systematically shift as a function of sleep stage, which has recently been shown to differ across development[4]. However, it is unknown whether there are region-specific differences in sleep-based aperiodic activity, whether these regional differences relate to the development of higher-order cognition and whether sleep-based and wake-based aperiodic activity change concomitantly.
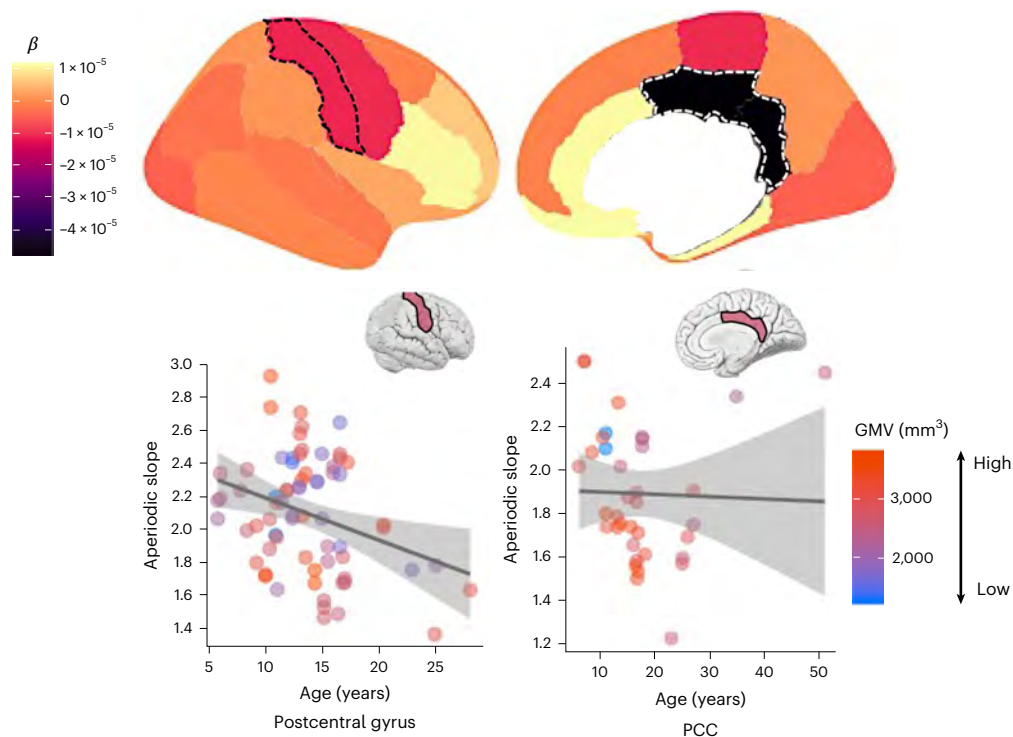
Fig. 7 | Regions with a significant interaction between age and GMV on the aperiodic slope. Top row: brain-wide GMV and age interactions on regional aperiodic slopes. Regions with statistically significant interactions between age and GMV (FDR <0.05) are indicated by dashed borders. Bottom row: scatter plots illustrating interactions between age (x axis; in years) and GMV (z scale; warmer colours denote higher GMV) on the aperiodic slopes (y axis; higher values denote a steeper slope) in regions with statistically significant interactions. Individual data points represent single participant data averaged across channels for each representative ROI. Shading shows the standard error.

Table 1 | Summary of main statistical tests including number of models computed, outcome variables, fixed effects and random effects

Analysis	Number of models	Type	Outcome	Fixed effects	Random effects	FDR
Association versus sensorimotor	1	Nonlinear mixed-effects regression	Slope	(1) Age (continuous; one spline, two knots) (2) Cortex type (categorical)	(1) Participant (intercept) (2) ROI (intercept) (3) Channel (nested under participant)	No
Attentional state	21	Linear mixed-effects regression	Slope	(1) Age (continuous) (2) Condition (categorical)	(1) Participant (intercept) (2) Channel (nested under participant) (3) Task (intercept)	Yes
Memory (task-based)	21	General linear regression	Accuracy	(1) Age (continuous) (2) Slope (continuous)	NA	Yes
Memory (task-free)	21	General linear regression	Accuracy	(1) Age (continuous) (2) Slope (continuous)	NA	Yes
GMV	20	Linear mixed-effects regression	Slope	(1) Age (continuous) (2) GMV (continuous)	(1) Participant (intercept) (2) Channel (nested under participant) (3) Task (intercept)	Yes

'Number of models' refers to the number of models performed for each analysis; 'Outcome' is the dependent variable; 'Cortex type' has two levels of association and sensorimotor; 'Condition' has two levels of task-free and task-based; false discovery rate (FDR) corrections were applied to all analyses apart from 'Association versus sensorimotor', given that one model was computed.

Implications

Historically, neuroscientific research has predominantly focused on young adults aged 18–40 years, largely overlooking the influence of age on brain dynamics. This practice has resulted in a significant knowledge gap regarding brain development. Addressing this gap is crucial due to its profound clinical implications across various domains, including neurodevelopmental disorders, traumatic brain injury, stroke, age-related cognitive decline and neurodegenerative diseases, as well as advancements in neural prosthetics for injury, stroke or disease management. Our study addresses this knowledge gap by elucidating the trajectory of aperiodic slopes and their associations with brain structure and memory across development, from childhood into late middle adulthood. Previous attempts to characterize these dynamics have been constrained by limitations in imprecise spatiotemporal measurements and relatively small sample sizes. To overcome these challenges, we adopted a comprehensive approach. First, we used iEEG to delineate developmental neurophysiology with exceptional precision. Second, we applied sophisticated analyses of aperiodic components in iEEG data to establish novel connections between aperiodic activity and developmental variations in memory. Third, we explored the relationship between aperiodic components and GMV. Lastly, we leveraged an exceptionally large iEEG dataset to detect subtle effects that may have been undetected in smaller cohorts.
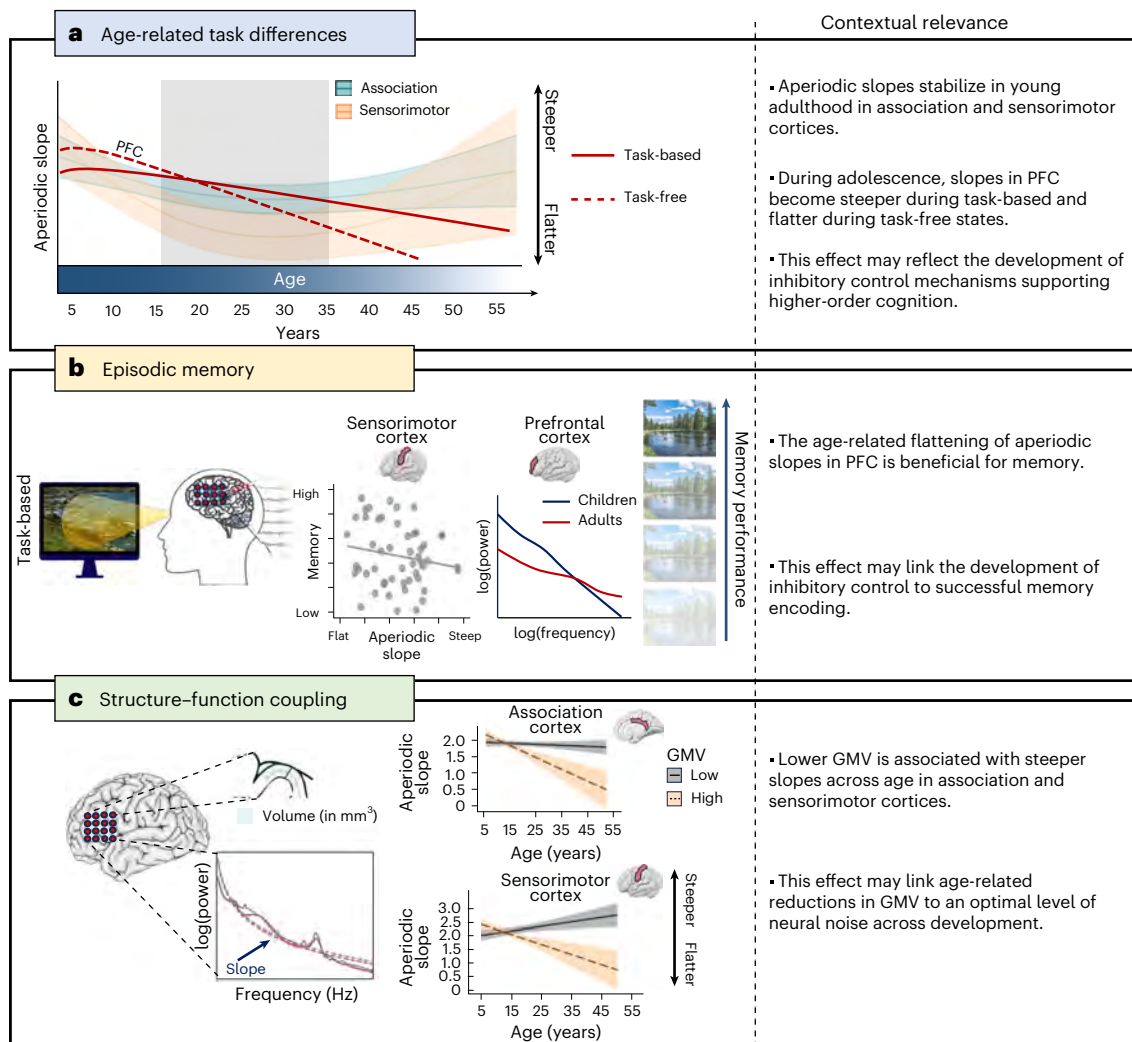
Fig. 8 | Aperiodic activity stabilizes in young adulthood, differs by age and attentional state, predicts age-related variability in episodic memory and is associated with age-related variability in GMV. a, Aperiodic slopes in sensorimotor (orange) and association (teal) cortices flatten from age 5 to 25 years and steepen thereafter. Note that the flattening is more pronounced in sensorimotor than association cortices in adolescence and young adulthood (grey shading). Regarding attentional state (that is, task-based versus task-free) differences in aperiodic activity, in the PFC, task-free (dashed red) slopes are steeper (that is, less neural noise) than task-based (solid red) slopes in children, and the inverse is observed in adults. Effects reverse at ~18–20 years of age, probably reflecting the development of control. Shading indicates

83% CIs. **b**, PFC-derived aperiodic slopes during task-based but not task-free states predicted age-related variability in memory performance, whereby the age-related flattening of aperiodic slopes was associated with age-related improvements in memory. Flatter sensorimotor cortical slopes were not associated with better memory performance after accounting for age. **c**, Modelling the relationship between brain volume and aperiodic slopes revealed similar age-related differences in structure–function coupling. In both the PCC and the postcentral gyrus, slopes were steeper in childhood regardless of GMV; in adolescence and adulthood, lower GMV was associated with steeper slopes and higher GMV was associated with flatter slopes. Shading indicates 83% CIs.

Understanding how cortical maturation influences memory encoding processes is also fundamental to cognitive function and daily performance, given well-documented changes in brain structure and function over the lifespan. Furthermore, elucidating the impact of brain development on memory formation across different life stages holds promise for early detection and intervention strategies targeting the emergence of both neurodevelopmental disorders and age-related memory decline. Identifying markers of healthy brain development and ageing is crucial for detecting dysfunction in age-related pathologies, which often manifest gradually over many years before exhibiting overt behavioural symptoms[103,104]. In this context, our findings may contribute to the prevention or delay of pathological ageing, offering significant health benefits, particularly considering the limitations and risks associated with current pharmacological treatments. Furthermore, our study lays the groundwork for

investigating memory dysfunction in psychiatric disorders, many of which emerge during adolescence and young adulthood, and which show deviations in aperiodic activity from healthy populations[23–26].

Conclusions

We reveal that aperiodic neural activity follows the same developmental time course across young adulthood in both sensorimotor and association cortices, challenging models of early sensorimotor development based on measures of brain structure. We also isolate attentional state and age-related differences in the aperiodic slope to the PFC, demonstrating that task-based slopes are steeper, reflecting less neural noise, and that this difference emerges during adolescence. We further establish the functional role of PFC-derived slopes in memory, revealing that age-related improvements in memory outcomes are associated with the age-related flattening of aperiodic slopes. Lastly, we characterized

the relationship between age-related differences in aperiodic activity and brain structure, identifying region-specific trajectories in structure–function relationships during development. Taken together, our findings establish brain-wide maps in aperiodic neural activity, its relation to age-related variability in memory and novel structure–function relationships, findings that are critical for understanding brain development and ageing in both health and disease.

Methods

Participants
The participants were 101 neurosurgical patients aged 5.93–54.00 years (63 males; mean age 19.25 years) undergoing iEEG monitoring as part of clinical seizure management. Patients with major lesions, prior surgical resections, noted developmental delays or neuropsychological memory test scores <80 were considered ineligible. Patients were recruited from Northwestern Memorial Hospital, the Ann & Robert H. Lurie Children's Hospital of Chicago, the Children's Hospital of Michigan, the University of California (UC), San Diego Rady Children's Hospital, UC Irvine Medical Center, UC Davis Medical Center, UC San Francisco Medical Center, Mount Sinai Hospital, California Pacific Medical Center, St. Louis Children's Hospital and Nationwide Children's Hospital. The institutional review boards of Northwestern University (no. STU00215843), Lurie Children's Hospital (no. 2022-5020), Wayne State University (no. 048404MP2E), UC Irvine and UC San Diego (no. 2014-1522), UC Davis (no. 1623773-1), UC San Francisco (no. 10-03842), Mount Sinai (no. STUDY-22-00529), California Pacific Medical Center (no. 666687-17), Washington University in St. Louis (no. 201102222) and the Nationwide Children's Hospital (no. 2020N0022) approved the study in accordance with the Declaration of Helsinki. Written informed consent was obtained from participants aged 18 years and older and from the guardians of participants aged under 18 years. Written assent was obtained from participants aged 13–17 years, and oral assent was obtained from younger children.

Given that electrode positioning in these participants was based on clinical necessity rather than for experimental reasons, a priori power analyses were not performed. Human iEEG research is limited by the availability of neurosurgical patients. From this perspective, the majority of iEEG work has been based on relatively small sample sizes and could not consider age-related or other sources of interindividual variability[41].

Experimental design
Task-based iEEG data were derived from the encoding phase of two visual memory recognition tasks that have been used extensively to study memory in adults and children across neuroimaging modalities, including iEEG. In the blocked-trial paradigm, participants encode a set of 40 indoor and outdoor scenes and classify each as indoor or outdoor in preparation for a self-paced old/new recognition test of all 40 studied scenes intermixed with 20 new scenes as foils[33,39,40,42–44,61,105–107]. In the single-trial paradigm, participants encode three shapes in a specific spatiotemporal sequence in preparation for a self-paced old/new recognition test of sequences that match exactly or mismatch on one dimension (that is, shape identity, spatial position or temporal order; cf. refs. [108–113]). Both paradigms use visual stimuli to avoid potential confounds on memory with verbal material in children and were presented using Psychtoolbox v.3.0.14. The encoding phases of the two paradigms are similar because, in both paradigms, participants encode visual stimuli (3,000 ms, 500–1,500 ms intertrial interval) in preparation for a self-paced, two-alternative forced-choice recognition test. We ensured that task-based data reflected task engagement by analysing only iEEG data recorded during the viewing of stimuli that were attended during encoding, as indexed by a correct indoor/outdoor classification of each scene in the blocked-trial paradigm and correct old/new classification of each sequence in the single-trial paradigm[39,40,42,43]. For a schematic of both visual memory tasks, see

Supplementary Fig. 14. For task-free data, participants were instructed to sit quietly with their eyes open, fixating on the centre of a computer monitor for 5 min. If no formal task-free task was administered, 5 min of task-free data were taken from natural rest in continuous 24/7 iEEG recordings. This occurred for 27 participants.

Behavioural analysis
Both visual memory tasks test memory in a two-alternative forced-choice design, permitting the use of similar measures of memory performance across tasks. For both tasks, for all participants, we calculated the hit rate (that is, the number of previously studied stimuli that were correctly recognized as old/match out of all studied stimuli) and false alarm rate (number of new stimuli presented that were incorrectly identified as 'old' or 'match' out of all 'new' or 'mismatched' stimuli). Performance accuracy was calculated as the hit rate minus the false alarm rate to equate measures across memory tasks and correct for differences in an individual's tendency to respond 'old'/'match' or 'new'/'mismatch', respectively. For a summary of behavioural performance, see Fig. 1c.

iEEG acquisition and preprocessing
iEEG data were recorded at a sampling rate of 200–5,000 Hz using Nihon Kohden JE120 Neurofax or Natus Quantum LTM recording systems, which at two sites were interfaced with the BCI2000 software. Data acquired >1,000 Hz were resampled to 1,000 Hz after the fact. As described below, spectral analysis was performed up to 60 Hz. Thus, the lowest sampling rate of 200 is well over the minimum Nyquist frequency required for analysis (that is, 2 cycles/frequency = 120 Hz). For consistency, all data from both visual memory tasks and from task-free recordings were preprocessed using the same procedures. Raw electrophysiological data were filtered with 0.1-Hz high-pass and 300-Hz low-pass finite impulse response filters, and 60-Hz line noise harmonics were removed using a discrete Fourier transform. Task-based continuous data were demeaned and epoched into 3-s trials (that is, 0–3 s from scene or study sequence onset). Continuous task-free data were also demeaned and transformed into 3-s epochs with 25% overlap. All epoched data were manually inspected blind to electrode locations and experimental task parameters. Electrodes overlying seizure onset zones and electrodes and epochs displaying epileptiform activity or artefactual signal (from poor contact, machine noise and so on) were excluded (mean proportion of rejected epochs 16.96%, s.d. 12.51). We used a bipolar re-referencing strategy, which has been shown to minimize the impact of impedance and electrode size differences between stereoelectroencephalography (sEEG) and electrocorticography (ECoG) and, thus, maximize standardization across these two types of recordings[114]. Neighbouring electrodes within the same anatomical structure were re-referenced using consistent conventions (ECoG, anterior–posterior; sEEG, deep–surface). For ECoG grids, electrodes were referenced to neighbouring electrodes on a row-by-row basis. An electrode was discarded if it did not have an adjacent neighbour, its neighbour was in a different anatomical structure, or both it and its neighbour were in white matter. Bipolar referencing yielded virtual channels that were located midway between the original physical electrodes. Data were then manually reinspected to reject any trials with residual noise. Preprocessing routines used functions from the FieldTrip toolbox for MATLAB[115]. All results were based on analysis of non-pathologic, artefact-free channels, ensuring that data represented healthy cortical tissue[116].

Aperiodic neural activity
The irregular-resampling auto-spectral analysis method[9] (IRASA) was used to estimate the $1/f$ power-law exponent. IRASA estimates the aperiodic component of neural time series data by resampling the signal at multiple non-integer factors h and their reciprocals $1/h$. As this resampling procedure systematically shifts narrowband peaks

away from their original location along the frequency spectrum, averaging the spectral densities of the resampled series attenuates peak components while preserving the 1/f distribution. The exponent summarizing the slope of aperiodic spectral activity is then calculated by fitting a linear regression in log–log space. Using the YASA toolbox[117] v.0.6.3, we fit a power-law function to each epoch within the frequency range of 1–60 Hz. For each epoch, channel and task, the inverse slope of the power-law function was taken as the trial-level estimate of the 1/f exponent.

iEEG localization

Macro-electrodes were surgically implanted for extraoperative recording based solely on clinical need. The electrodes were subdural electrode grids or strips with 10-mm spacing or sEEG electrodes with 5–10 mm spacing. Anatomical locations were determined by co-registering postimplantation computed tomography coordinates to preoperative magnetic resonance images, as implemented in FieldTrip[118], FreeSurfer[119], iELVis[120] or VERA[121]. Electrode locations were then projected into standard Montreal Neurological Institute (MNI) space and bipolar channel locations (see preprocessing) were projected at the midpoint between their contributing electrodes. Based on these MNI coordinates, the R package label4MRI v1.2 (https://github.com/yunshiuan/label4MRI) was used to categorize each channel into its corresponding Brodmann area, which were then grouped according to the DKT atlas[64].

Structural imaging and regional GMV

T1-weighted MRI scans were acquired as part of routine preoperative procedures. Parcellation of cortex into ROIs was performed on the basis of standard procedures implemented within FreeSurfer[119]. Regional GMVs were then estimated on the basis of the DKT atlas[64]. GMV from each ROI was calculated using FreeSurfer[119]. Volumes were calculated for left and right ROIs and averaged across hemispheres for analysis.

Statistical analysis

Data were imported into R version 4.2.3 with the aid of the tidyverse package[122] and analysed using linear and nonlinear mixed-effects models fit by restricted maximum likelihood using lme4[123] and splines. P values for region-specific models were estimated using the summary function from the lmerTest package, which is based on Satterthwaite's degrees of freedom[123], and type II Wald tests from the car package[124] for examination of whole-brain effects (that is, models that included all ROIs). Effects were plotted using the package ggeffects[125] and ggplot2[126]. Spearman correlations were used to assess structure–function relationships without the effect of age, with coefficients used to plot region-specific relationships between aperiodic activity and GMV across the whole brain. Statistical significance was adjusted using the false discovery rate with an alpha threshold of 0.05. Task was entered as an unordered factor using sum-to-zero contrast coding, and age was specified as a continuous predictor. Please see Table 1 for a summary of the main analyses, including the types of models used and their fixed and random effects structures.

In our preregistration, we specified that we would apply a spline to age to model potential nonlinear effects of age on aperiodic activity for each ROI, as well as a random effect of task-free recording type (eyes open versus eyes closed). However, in doing so, models indicated non-convergence or singular fit. To reduce model complexity, we modelled age as a linear predictor and removed task-free recording type as a random effect in our analysis of each ROI. For analyses testing hypotheses (a) and (b), where we tested differences in association and sensorimotor cortices, we had sufficient power to model nonlinear differences. Specifically, we used linear mixed-effects models with a single spline with two internal knots on age specified using the splines package. The model uses a natural spline with two degrees of freedom, which

corresponds to a single spline with two knots. This spline approach allows for a nonlinear relationship between age and the aperiodic slope by dividing the age range into three segments. The choice of two knots reflects a balance between flexibility and model complexity, ensuring that we can model age-related differences without introducing excessive parameters. This approach enables the model to capture potential nonlinear patterns in the data, which is necessary to test our hypotheses that slopes would vary by age in childhood and then stabilize in adolescence or adulthood. To determine whether there were differences between spline choices, we ran the same model but with a spline with three internal knots. Comparing the fits between the model with two and three knots did not reveal a significant difference in model fit indices ($P > 0.05$).

When contrast coding is explicitly described, the need for post-hoc testing is eliminated (for a detailed discussion of contrast coding in linear mixed-effects regressions, see ref. 127). Furthermore, for modelled effects, an 83% CI threshold was used, given that this approach corresponds to the 5% significance level with non-overlapping estimates[128,129]. To isolate outliers for variables that were specified as outcomes (that is, aperiodic slopes, memory performance), we used Tukey's method[130], which identifies outliers as exceeding ±1.5× interquartile range. The packages ggseg[131] and ggsegDKT were used to generate cortical plots based on DKT atlas nomenclature. Hypotheses (a) and (b) were tested using the following formula (note that, in all models, asterisks denote interaction terms, plus signs denote additive terms, B_0 denotes the intercept of the model, and B_1, B_2 and so on denote the chronological specification of fixed effect parameters):

$$\text{EEG}_i = \beta_0 + \beta_1 ns\,(\text{age}, 2)_i * \beta_2 \text{region}_i + \text{channel/subject}_{0i} + \epsilon,$$

where EEG is the aperiodic slope; age is age in years modelled with one natural spline term (ns) with two internal knots; region encodes association and sensorimotor cortices; channel encodes region-specific channels nested under the random intercept of participant; and participant is the random intercept term of participant ID. To test hypothesis (c), we used the following model equation on a region-by-region basis:

$$\text{EEG}_i = \beta_0 + \beta_1 \text{condition}_i * \beta_2 \text{age}_i + \text{channel/subject}_{0i} + \text{task}_{0i} + \epsilon,$$

where EEG is the aperiodic slope; condition encodes task-based and task-free recordings; age is age in years modelled as a linear predictor; channel encodes region-specific channels nested under participant; and participant is participant ID, while task is a random intercept encoding whether the recording is derived from the blocked or single-trial memory task.

Our exploratory analyses focused on relationships between GMV, behavioural performance and aperiodic slopes derived from task-based and task-free recordings. Here, our primary exploratory research questions were whether

(1) regional age-related variability in aperiodic slopes predicts variability in memory performance, and;
(2) regional age-related variability in GMV predicts variability in aperiodic slopes.

These exploratory analyses were examined with general linear models with the following formulae:

$$(\text{a})\ \text{memory}_i = \beta_0 + \beta_1 \text{age}_i * \beta_2 \text{EEG}_i + \epsilon,$$

where memory is performance on the visual memory task(s); age is age in years modelled as a linear predictor; and EEG is the aperiodic slope from each ROI.

$$(\text{b})\ \text{EEG}_i = \beta_0 + \beta_1 \text{age}_i * \beta_2 \text{volume}_i + \text{channel/subject}_{0i} + \text{task}_{0i} + \epsilon,$$

where EEG is the aperiodic slope; age is age in years modelled as a linear predictor; volume is regional GMV in mm³; channel encodes ROI-specific channels; participant is the participant ID; and task encodes whether the task recording was from the blocked or single-trial memory task. As with the other models, each ROI was applied to the model equation described above. Participant was modelled as a random effect on the intercept, while channel was nested under participant. Task was also specified as a random effect on the intercept. Note that, in our preregistration, we stated that we would include task (task-based, task-free) in all models examining the interaction between GMV and age on aperiodic activity. However, all models indicated non-convergence or singular fits. To reduce model complexity, we examined aperiodic activity during task-based states only.

Reporting summary

Further information on research design is available in the Nature Portfolio Reporting Summary linked to this article.

Data availability

All data and code are available at https://tinyurl.com/m5yfc9ny.

References

1. Bethlehem, R. A. I. et al. Brain charts for the human lifespan. *Nature* **604**, 525–533 (2022).
2. Gogtay, N. et al. Dynamic mapping of human cortical development during childhood through early adulthood. *Proc. Natl Acad. Sci. USA* **101**, 8174–8179 (2004).
3. Grydeland, H. et al. Waves of maturation and senescence in micro-structural MRI markers of human cortical myelination over the lifespan. *Cereb. Cortex* **29**, 1369–1381 (2019).
4. Favaro, J. et al. The maturation of aperiodic EEG activity across development reveals a progressive differentiation of wakefulness from sleep. *NeuroImage* **277**, 120264 (2023).
5. Hill, A. T., Clark, G. M., Bigelow, F. J., Lum, J. A. G. & Enticott, P. G. Periodic and aperiodic neural activity displays age-dependent changes across early-to-middle childhood. *Dev. Cogn. Neurosci.* **54**, 101076 (2022).
6. Schaworonkow, N. & Voytek, B. Longitudinal changes in aperiodic and periodic activity in electrophysiological recordings in the first seven months of life. *Dev. Cogn. Neurosci.* **47**, 100895 (2021).
7. Tröndle, M., Popov, T., Dziemian, S. & Langer, N. Decomposing the role of alpha oscillations during brain maturation. *eLife* **11**, e77571 (2022).
8. Donoghue, T. et al. Parameterizing neural power spectra into periodic and aperiodic components. *Nat. Neurosci.* **23**, 1655–1665 (2020).
9. Wen, H. & Liu, Z. Separating fractal and oscillatory components in the power spectrum of neurophysiological signal. *Brain Topogr.* **29**, 13–26 (2016).
10. Ahmad, J. et al. From mechanisms to markers: novel noninvasive EEG proxy markers of the neural excitation and inhibition system in humans. *Transl. Psychiatry* **12**, 467 (2022).
11. van Nifterick, A. M. et al. Resting-state oscillations reveal disturbed excitation–inhibition ratio in Alzheimer's disease patients. *Sci. Rep.* **13**, 7419 (2023).
12. Manning, J. R., Jacobs, J., Fried, I. & Kahana, M. J. Broadband shifts in local field potential power spectra are correlated with single-neuron spiking in humans. *J. Neurosci.* **29**, 13613–13620 (2009).
13. Miller, K. J. et al. Human motor cortical activity is selectively phase-entrained on underlying rhythms. *PLoS Comput. Biol.* **9**, e1002655 (2012).
14. Kramer, M. A. & Chu, C. J. A general, noise-driven mechanism for the 1/f-like behavior of neural field spectra. *Neural Comput.* **36**, 1643–1668 (2024).
15. Voytek, B. & Knight, R. T. Dynamic network communication as a unifying neural basis for cognition, development, aging, and disease. *Biol. Psychiatry* **77**, 1089–1097 (2015).
16. Voytek, B. et al. Age-related changes in 1/f neural electrophysiological noise. *J. Neurosci.* **35**, 13257–13265 (2015).
17. Buzsáki, G., Anastassiou, C. A. & Koch, C. The origin of extracellular fields and currents—EEG, ECoG, LFP and spikes. *Nat. Rev. Neurosci.* **13**, 407–420 (2012).
18. Bédard, C. & Destexhe, A. Macroscopic models of local field potentials and the apparent 1/f noise in brain activity. *Biophys. J.* **96**, 2589–2603 (2009).
19. Evertz, R., Hicks, D. G. & Liley, D. T. Alpha blocking and 1/fβ spectral scaling in resting EEG can be accounted for by a sum of damped alpha band oscillatory processes. *PLoS Comput. Biol.* **18**, e1010012 (2022).
20. Martínez-Cañada, P. et al. Combining aperiodic 1/f slopes and brain simulation: an EEG/MEG proxy marker of excitation/inhibition imbalance in Alzheimer's disease. *Alzheimers Dement. Diagn. Assess. Dis. Monit.* **15**, e12477 (2023).
21. Wiest, C. et al. The aperiodic exponent of subthalamic field potentials reflects excitation/inhibition balance in Parkinsonism. *eLife* **12**, e82467 (2023).
22. Turrigiano, G. G. & Nelson, S. B. Homeostatic plasticity in the developing nervous system. *Nat. Rev. Neurosci.* **5**, 97–107 (2004).
23. Earl, R. J., Ford, T. C., Lum, J. A. G., Enticott, P. G. & Hill, A. T. Exploring aperiodic activity in first episode schizophrenia spectrum psychosis: a resting-state EEG analysis. *Brain Res.* **1840**, 149052 (2024).
24. Pani, S. M., Saba, L. & Fraschini, M. Clinical applications of EEG power spectra aperiodic component analysis: a mini-review. *Clin. Neurophysiol.* **143**, 1–13 (2022).
25. Shuffrey, L. C. et al. Aperiodic electrophysiological activity in preterm infants is linked to subsequent autism risk. *Dev. Psychobiol.* **64**, e22271 (2022).
26. Fernandez, F. & Garner, C. C. Over-inhibition: a model for developmental intellectual disability. *Trends Neurosci.* **30**, 497–503 (2007).
27. Merkin, A. et al. Do age-related differences in aperiodic neural activity explain differences in resting EEG alpha? *Neurobiol. Aging* **121**, 78–87 (2023).
28. Waschke, L., Wöstmann, M. & Obleser, J. States and traits of neural irregularity in the age-varying human brain. *Sci. Rep.* **7**, 17381 (2017).
29. Tran, T. T., Rolle, C. E., Gazzaley, A. & Voytek, B. Linked sources of neural noise contribute to age-related cognitive decline. *J. Cogn. Neurosci.* **32**, 1813–1822 (2020).
30. Cross, Z. R., Corcoran, A. W., Schlesewsky, M., Kohler, M. J. & Bornkessel-Schlesewsky, I. Oscillatory and aperiodic neural activity jointly predict language learning. *J. Cogn. Neurosci.* **34**, 1630–1649 (2022).
31. Lendner, J. D. et al. Oscillatory and aperiodic neuronal activity in working memory following anesthesia. *Clin. Neurophysiol.* **150**, 79–88 (2023).
32. Cellier, D., Riddle, J., Petersen, I. & Hwang, K. The development of theta and alpha neural oscillations from ages 3 to 24 years. *Dev. Cogn. Neurosci.* **50**, 100969 (2021).
33. Ofen, N., Tang, L., Yu, Q. & Johnson, E. L. Memory and the developing brain: from description to explanation with innovation in methods. *Dev. Cogn. Neurosci.* **36**, 100613 (2019).
34. Musall, S., von Pföstl, V., Rauch, A., Logothetis, N. K. & Whittingstall, K. Effects of neural synchrony on surface EEG. *Cereb. Cortex* **24**, 1045–1053 (2014).
35. Palva, J. M. et al. Ghost interactions in MEG/EEG source space: a note of caution on inter-areal coupling measures. *NeuroImage* **173**, 632–643 (2018).

36. Johnson, E. L., Kam, J. W., Tzovara, A. & Knight, R. T. Insights into human cognition from intracranial EEG: a review of audition, memory, internal cognition, and causality. *J. Neural Eng.* **17**, 051001 (2020).

37. Johnson, E. L. & Knight, R. T. Intracranial recordings and human memory. *Curr. Opin. Neurobiol.* **31**, 18–25 (2015).

38. Parvizi, J. & Kastner, S. Promises and limitations of human intracranial electroencephalography. *Nat. Neurosci.* **21**, 474–483 (2018).

39. Johnson, E. L., Tang, L., Yin, Q., Asano, E. & Ofen, N. Direct brain recordings reveal prefrontal cortex dynamics of memory development. *Sci. Adv.* **4**, eaat3702 (2018).

40. Johnson, E. L. et al. Dissociable oscillatory theta signatures of memory formation in the developing brain. *Curr. Biol.* **32**, 1457–1469.e4 (2022).

41. Johnson, E. L. & Knight, R. T. How can iEEG be used to study inter-individual and developmental differences? in *Intracranial EEG: A Guide for Cognitive Neuroscientists* (ed Axmacher, N.) 143–154 (Springer, 2023).

42. Rau, E. M. B. et al. Reinstatement and transformation of memory traces for recognition. *Sci. Adv.* **11**, eadp9336 (2025).

43. Yin, Q. et al. Direct brain recordings reveal occipital cortex involvement in memory development. *Neuropsychologia* **148**, 107625 (2020).

44. Yin, Q., Johnson, E. L. & Ofen, N. Neurophysiological mechanisms of cognition in the developing brain: Insights from intracranial EEG studies. *Dev. Cogn. Neurosci.* **64**, 101312 (2023).

45. Leszczyński, M. et al. Dissociation of broadband high-frequency activity and neuronal firing in the neocortex. *Sci. Adv.* **6**, eabb0977 (2020).

46. Nir, Y. et al. Coupling between neuronal firing rate, gamma LFP, and BOLD fMRI is related to interneuronal correlations. *Curr. Biol.* **17**, 1275–1285 (2007).

47. Ray, S., Crone, N. E., Niebur, E., Franaszczuk, P. J. & Hsiao, S. S. Neural correlates of high-gamma oscillations (60–200 Hz) in macaque local field potentials and their potential implications in electrocorticography. *J. Neurosci.* **28**, 11526–11536 (2008).

48. Rich, E. L. & Wallis, J. D. Spatiotemporal dynamics of information encoding revealed in orbitofrontal high-gamma. *Nat. Commun.* **8**, 1139 (2017).

49. Watson, B. O., Ding, M. & Buzsáki, G. Temporal coupling of field potentials and action potentials in the neocortex. *Eur. J. Neurosci.* **48**, 2482–2497 (2018).

50. Hunt, B. A. et al. Relationships between cortical myeloarchitecture and electrophysiological networks. *Proc. Natl Acad. Sci. USA* **113**, 13510–13515 (2016).

51. Schölvinck, M. L., Leopold, D. A., Brookes, M. J. & Khader, P. H. The contribution of electrophysiology to functional connectivity mapping. *NeuroImage* **80**, 297–306 (2013).

52. Doval, S. et al. When maturation is not linear: brain oscillatory activity in the process of aging as measured by electrophysiology. *Brain Topogr.* https://doi.org/10.1007/s10548-024-01064-0 (2024).

53. Overbye, K., Huster, R. J., Walhovd, K. B., Fjell, A. M. & Tamnes, C. K. Development of the P300 from childhood to adulthood: a multimodal EEG and MRI study. *Brain Struct. Funct.* **223**, 4337–4349 (2018).

54. Sui, J., Huster, R., Yu, Q., Segall, J. & Calhoun, V. Function–structure associations of the brain: evidence from multimodal connectivity and covariance studies. *NeuroImage* **102**, 11–23 (2014).

55. Whitford, T. J. et al. Brain maturation in adolescence: concurrent changes in neuroanatomy and neurophysiology. *Hum. Brain Mapp.* **28**, 228–237 (2007).

56. Groeschel, S., Vollmer, B., King, M. & Connelly, A. Developmental changes in cerebral grey and white matter volume from infancy to adulthood. *Int. J. Dev. Neurosci.* **28**, 481–489 (2010).

57. Finley, A. J., Angus, D. J., Van Reekum, C. M., Davidson, R. J. & Schaefer, S. M. Periodic and aperiodic contributions to theta-beta ratios across adulthood. *Psychophysiology* **59**, e14113 (2022).

58. Thuwal, K., Banerjee, A. & Roy, D. Aperiodic and periodic components of ongoing oscillatory brain dynamics link distinct functional aspects of cognition across adult lifespan. *eNeuro* https://doi.org/10.1523/eneuro.0224-21.2021 (2021).

59. Hill, J. et al. Similar patterns of cortical expansion during human development and evolution. *Proc. Natl Acad. Sci. USA* **107**, 13135–13140 (2010).

60. Sydnor, V. J. et al. Neurodevelopment of the association cortices: patterns, mechanisms, and implications for psychopathology. *Neuron* **109**, 2820–2846 (2021).

61. Ofen, N. et al. Development of the declarative memory system in the human brain. *Nat. Neurosci.* **10**, 1198–1205 (2007).

62. Wilke, M., Krägeloh-Mann, I. & Holland, S. K. Global and local development of gray and white matter volume in normal children and adolescents. *Exp. Brain Res.* **178**, 296–307 (2007).

63. Hill, P. F., King, D. R., Lega, B. C. & Rugg, M. D. Comparison of fMRI correlates of successful episodic memory encoding in temporal lobe epilepsy patients and healthy controls. *NeuroImage* **207**, 116397 (2020).

64. Klein, A. & Tourville, J. 101 labeled brain images and a consistent human cortical labeling protocol. *Front. Neurosci.* **6**, (2012).

65. Fotiadis, P. et al. Myelination and excitation–inhibition balance synergistically shape structure-function coupling across the human cortex. *Nat. Commun.* **14**, 6115 (2023).

66. Mahjoory, K., Schoffelen, J.-M., Keitel, A. & Gross, J. The frequency gradient of human resting-state brain oscillations follows cortical hierarchies. *eLife* **9**, e53715 (2020).

67. Keller, A. S. et al. Hierarchical functional system development supports executive function. *Trends Cogn. Sci.* **27**, 160–174 (2023).

68. Larsen, B., Sydnor, V. J., Keller, A. S., Yeo, B. T. T. & Satterthwaite, T. D. A critical period plasticity framework for the sensorimotor–association axis of cortical neurodevelopment. *Trends Neurosci.* **46**, 847–862 (2023).

69. Sydnor, V. J. et al. Intrinsic activity development unfolds along a sensorimotor–association cortical axis in youth. *Nat. Neurosci.* **26**, 638–649 (2023).

70. Tervo-Clemmens, B. et al. A canonical trajectory of executive function maturation from adolescence to adulthood. *Nat. Commun.* **14**, 6922 (2023).

71. Momi, D. et al. Stimulation mapping and whole-brain modeling reveal gradients of excitability and recurrence in cortical networks. *Nat. Commun.* **16**, 3222 (2025).

72. Bornkessel-Schlesewsky, I. et al. Effects of neural noise on predictive model updating across the adult lifespan. Preprint at *bioRxiv* https://doi.org/10.1101/2022.12.14.520501 (2022).

73. McSweeney, M. et al. Age-related trends in aperiodic EEG activity and alpha oscillations during early- to middle-childhood. *NeuroImage* **269**, 119925 (2023).

74. Ouyang, G., Hildebrandt, A., Schmitz, F. & Herrmann, C. S. Decomposing alpha and 1/f brain activities reveals their differential associations with cognitive processing speed. *NeuroImage* **205**, 116304 (2020).

75. Gazit, T. et al. The role of mPFC and MTL neurons in human choice under goal-conflict. *Nat. Commun.* **11**, 3192 (2020).

76. Miller, E. K. & Cohen, J. D. An integrative theory of prefrontal cortex function. *Annu. Rev. Neurosci.* **24**, 167–202 (2001).

77. Noudoost, B. & Moore, T. Control of visual cortical signals by prefrontal dopamine. *Nature* **474**, 372–375 (2011).

78. Dave, S., Brothers, T. A. & Swaab, T. Y. 1/f neural noise and electrophysiological indices of contextual prediction in aging. *Brain Res.* **1691**, 34–43 (2018).

79. Sheehan, T. C., Sreekumar, V., Inati, S. K. & Zaghloul, K. A. Signal complexity of human intracranial EEG tracks successful associative-memory formation across individuals. *J. Neurosci.* **38**, 1744 (2018).

80. Immink, M. A. et al. Resting-state aperiodic neural dynamics predict individual differences in visuomotor performance and learning. *Hum. Mov. Sci.* **78**, 102829 (2021).

81. Dziego, C. A. et al. Neural and cognitive correlates of performance in dynamic multi-modal settings. *Neuropsychologia* **180**, 108483 (2023).

82. Fuster, J. M. Frontal lobe and cognitive development. *J. Neurocytol.* **31**, 373–385 (2002).

83. Ridderinkhof, K. R., Ullsperger, M., Crone, E. A. & Nieuwenhuis, S. The role of the medial frontal cortex in cognitive control. *Science* **306**, 443–447 (2004).

84. Robertson, M. M. et al. EEG power spectral slope differs by ADHD status and stimulant medication exposure in early childhood. *J. Neurophysiol.* **122**, 2427–2437 (2019).

85. Molina, J. L. et al. Memantine effects on electroencephalographic measures of putative excitatory/inhibitory balance in schizophrenia. *Biol. Psychiatry Cogn. Neurosci. Neuroimag.* **5**, 562–568 (2020).

86. Peterson, E. J., Rosen, B. Q., Belger, A., Voytek, B. & Campbell, A. M. Aperiodic neural activity is a better predictor of schizophrenia than neural oscillations. *Clin. EEG Neurosci.* **54**, 434–445 (2023).

87. Kolk, S. M. & Rakic, P. Development of prefrontal cortex. *Neuropsychopharmacology* **47**, 41–57 (2022).

88. McKeon, S. D. et al. Aperiodic EEG and 7T MRSI evidence for maturation of E/I balance supporting the development of working memory through adolescence. *Dev. Cogn. Neurosci.* **66**, 101373 (2024).

89. Sukenik, N. et al. Neuronal circuits overcome imbalance in excitation and inhibition by adjusting connection numbers. *Proc. Natl Acad. Sci. USA* **118**, e2018459118 (2021).

90. Bornkessel-Schlesewsky, I. et al. Rapid adaptation of predictive models during language comprehension: aperiodic EEG slope, individual alpha frequency and idea density modulate individual differences in real-time model updating. *Front. Psychol.* **13**, 817516 (2022).

91. Braver, T. S., Paxton, J. L., Locke, H. S. & Barch, D. M. Flexible neural mechanisms of cognitive control within human prefrontal cortex. *Proc. Natl Acad. Sci. USA* **106**, 7351–7356 (2009).

92. Cabeza, R. et al. Maintenance, reserve and compensation: the cognitive neuroscience of healthy ageing. *Nat. Rev. Neurosci.* **19**, 701–710 (2018).

93. Spreng, R. N. & Turner, G. R. The shifting architecture of cognition and brain function in older adulthood. *Perspect. Psychol. Sci.* **14**, 523–542 (2019).

94. Buzsaki, G. *Rhythms of the Brain* (Oxford Univ. Press, 2006).

95. Nunez, P. L. & Srinivasan, R. Recording strategies, reference issues, and dipole localization. *Nunez PL Srinivasan R. Electr. Fields Brain Neurophys. EEG Ed.* **2**, 275–312 (2006).

96. Euler, M. J. et al. Associations between the resting EEG aperiodic slope and broad domains of cognitive ability. *Psychophysiology* **61**, e14543 (2024).

97. Montemurro, S. et al. Aperiodic component of EEG power spectrum and cognitive performance are modulated by education in aging. *Sci. Rep.* **14**, 15111 (2024).

98. Pi, Y. et al. Interindividual aperiodic resting-state EEG activity predicts cognitive-control styles. *Psychophysiology* **61**, e14576 (2024).

99. Larsen, B. et al. A developmental reduction of the excitation:inhibition ratio in association cortex during adolescence. *Sci. Adv.* **8**, eabj8750 (2022).

100. Miller, K. J., Sorensen, L. B., Ojemann, J. G. & den Nijs, M. Power-law scaling in the brain surface electric potential. *PLoS Comput. Biol.* **5**, e1000609 (2009).

101. Herweg, N. A., Solomon, E. A. & Kahana, M. J. Theta oscillations in human memory. *Trends Cogn. Sci.* **24**, 208–227 (2020).

102. Lega, B. C., Jacobs, J. & Kahana, M. Human hippocampal theta oscillations and the formation of episodic memories. *Hippocampus* **22**, 748–761 (2012).

103. Josefsson, M. et al. Memory profiles predict dementia over 23–28 years in normal but not successful aging. *Int. Psychogeriatr.* **35**, 351–359 (2023).

104. Riley, K. P. et al. Prediction of preclinical Alzheimer's disease: longitudinal rates of change in cognition. *J. Alzheimer's Dis.* **25**, 707–717 (2011).

105. Chai, X. J., Ofen, N., Jacobs, L. F. & Gabrieli, J. D. Scene complexity: influence on perception, memory, and development in the medial temporal lobe. *Front. Hum. Neurosci.* **4**, 1021 (2010).

106. Ofen, N., Chai, X. J., Schuil, K. D., Whitfield-Gabrieli, S. & Gabrieli, J. D. The development of brain systems associated with successful memory retrieval of scenes. *J. Neurosci.* **32**, 10012–10020 (2012).

107. Tang, L., Shafer, A. T. & Ofen, N. Prefrontal cortex contributions to the development of memory formation. *Cereb. Cortex* **28**, 3295–3308 (2018).

108. Davoudi, S., Parto Dezfouli, M., Knight, R. T., Daliri, M. R. & Johnson, E. L. Prefrontal lesions disrupt posterior alpha–gamma coordination of visual working memory representations. *J. Cogn. Neurosci.* **33**, 1798–1810 (2021).

109. Dezfouli, M. P., Davoudi, S., Knight, R. T., Daliri, M. R. & Johnson, E. L. Prefrontal lesions disrupt oscillatory signatures of spatiotemporal integration in working memory. *Cortex* **138**, 113–126 (2021).

110. Johnson, E. L. et al. Dynamic frontotemporal systems process space and time in working memory. *PLoS Biol.* **16**, e2004274 (2018).

111. Johnson, E. L. et al. Orbitofrontal cortex governs working memory for temporal order. *Curr. Biol.* **32**, R410–R411 (2022).

112. Johnson, E. L. et al. Bidirectional frontoparietal oscillatory systems support working memory. *Curr. Biol.* **27**, 1829–1835 (2017).

113. Johnson, E. L. et al. Spectral imprints of working memory for everyday associations in the frontoparietal network. *Front. Syst. Neurosci.* **12**, 65 (2019).

114. Mercier, M. R. et al. Advances in human intracranial electroencephalography research, guidelines and good practices. *NeuroImage* **260**, 119438 (2022).

115. Oostenveld, R., Fries, P., Maris, E. & Schoffelen, J.-M. FieldTrip: open source software for advanced analysis of MEG, EEG, and invasive electrophysiological data. *Comput. Intell. Neurosci.* **2011**, 1–9 (2011).

116. Rossini, L. et al. Seizure activity per se does not induce tissue damage markers in human neocortical focal epilepsy. *Ann. Neurol.* **82**, 331–341 (2017).

117. Vallat, R. & Walker, M. P. An open-source, high-performance tool for automated sleep staging. *Elife* **10**, e70092 (2021).

118. Stolk, A. et al. Integrated analysis of anatomical and electrophysiological human intracranial data. *Nat. Protoc.* **13**, 1699–1723 (2018).

119. Fischl, B. FreeSurfer. *NeuroImage* **62**, 774–781 (2012).

120. Groppe, D. M. et al. iELVis: An open source MATLAB toolbox for localizing and visualizing human intracranial electrode data. *J. Neurosci. Methods* **281**, 40–48 (2017).

121. Adamek, M., Swift, J. R. & Brunner, P. VERA-Versatile electrode localization Framework. *Zenodo* https://doi.org/10.5281/zenodo.7486841 (2022).

122. Wickham, H. et al. Welcome to the Tidyverse. *J. Open Source Softw.* **4**, 1686 (2019).

123. Kuznetsova, A., Brockhoff, P. B. & Christensen, R. H. lmerTest package: tests in linear mixed effects models. *J. Stat. Softw.* **82**, 1–26 (2017).

124. Fox, J. et al. The car package. *R. Found. Stat. Comput.* **1109**, 1431 (2007).
125. Lüdecke, D. ggeffects: Tidy data frames of marginal effects from regression models. *J. Open Source Softw.* **3**, 772 (2018).
126. Wickham, H. *ggplot2: Elegant Graphics for Data Analysis* (Springer-Verlag, 2016).
127. Brehm, L. & Alday, P. M. Contrast coding choices in a decade of mixed models. *J. Mem. Lang.* **125**, 104334 (2022).
128. Austin, P. C. & Hux, J. E. A brief note on overlapping confidence intervals. *J. Vasc. Surg.* **36**, 194–195 (2002).
129. MacGregor-Fors, I. & Payton, M. E. Contrasting diversity values: statistical inferences based on overlapping confidence intervals. *PLoS ONE* **8**, e56794 (2013).
130. Tukey, J. W. *Exploratory Data Analysis* Vol. 2 131–160 (Addison-Wesley, 1977).
131. Mowinckel, A. M. & Vidal-Piñeiro, D. Visualization of brain statistics with R packages ggseg and ggseg3d. *Adv. Methods Pract. Psychol. Sci.* **3**, 466–483 (2020).

Acknowledgements

Author contributions

Z.R.C., N.O. and E.L.J. designed the study. S.M.G., A.J.O.D., Y.M.R., C.R., A.M.H., E.A., J.J.L., O.K.M., S.S., I.S., F.G., D.K.-S., P.B.W., K.D.L., S.U.S., J.M.R., J.Y.W., S.K.L., J.S.R., E.F.C., A.S., P.B., J.L.R., R.M.B. and E.L.J. recruited patients and/or collected data. Z.R.C., S.M.G., Q.Y., P.V., E.M.B.R., C.C., A.M.H., R.T.K., N.O. and E.L.J. preprocessed data. Z.R.C. and A.J.O.D. analysed data. Z.R.C. visualized results. Z.R.C. and E.L.J. interpreted data. Z.R.C. drafted the manuscript. Z.R.C. and E.L.J. revised the manuscript. E.L.J. supervised the study. All authors provided feedback on the completed manuscript.

Competing interests

The authors declare no competing interests.

Additional information

Supplementary information The online version contains supplementary material available at https://doi.org/10.1038/s41562-025-02270-x.

Correspondence and requests for materials should be addressed to Zachariah R. Cross.

Peer review information *Nature Human Behaviour* thanks Aron Hill, Ezequiel Mikulan and the other, anonymous, reviewer(s) for their contribution to the peer review of this work. Peer reviewer reports are available.

Reprints and permissions information is available at www.nature.com/reprints.

Zachariah R. Cross [1] ✉, **Samantha M. Gray**[1,2], **Adam J. O. Dede**[1], **Yessenia M. Rivera**[1], **Qin Yin**[3,4], **Parisa Vahidi** [3], **Elias M. B. Rau** [5], **Christopher Cyr**[1], **Ania M. Holubecki** [1], **Eishi Asano** [3], **Jack J. Lin** [6], **Olivia Kim McManus** [7], **Shifteh Sattar**[7], **Ignacio Saez** [6,8], **Fady Girgis**[6,9], **David King-Stephens**[10,11], **Peter B. Weber** [10], **Kenneth D. Laxer**[10], **Stephan U. Schuele**[1], **Joshua M. Rosenow**[1], **Joyce Y. Wu**[1,12], **Sandi K. Lam**[1,12], **Jeffrey S. Raskin**[1,12], **Edward F. Chang** [13], **Ammar Shaikhouni**[14], **Peter Brunner**[15], **Jarod L. Roland** [15,16], **Rodrigo M. Braga** [1], **Robert T. Knight** [17], **Noa Ofen**[3,4] & **Elizabeth L. Johnson** [1]

[1]Northwestern University, Chicago, IL, USA. [2]Stanford University, Stanford, CA, USA. [3]Wayne State University, Detroit, MI, USA. [4]University of Texas, Dallas, Dallas, TX, USA. [5]Ruhr University Bochum, Bochum, Germany. [6]University of California, Davis, Davis, CA, USA. [7]University of California, San Diego, and Rady Children's Hospital, San Diego, CA, USA. [8]Ichan School of Medicine at Mount Sinai, New York City, NY, USA. [9]University of Calgary, Calgary, Alberta, Canada. [10]California Pacific Medical Center, San Francisco, CA, USA. [11]Yale University, New Haven, CT, USA. [12]Ann and Robert H. Lurie Children's Hospital of Chicago, Chicago, IL, USA. [13]University of California, San Francisco, San Francisco, CA, USA. [14]Ohio State University and Nationwide Children's Hospital, Columbus, OH, USA. [15]Washington University in St. Louis, St. Louis, MO, USA. [16]St. Louis Children's Hospital, St. Louis, MO, USA. [17]University of California, Berkeley, Berkeley, CA, USA. ✉e-mail: zachariah.cross@northwestern.edu

Corresponding author(s): Zachariah R. Cross

Last updated by author(s): May 28, 2025

Reporting Summary

Nature Portfolio wishes to improve the reproducibility of the work that we publish. This form provides structure for consistency and transparency in reporting. For further information on Nature Portfolio policies, see our Editorial Policies and the Editorial Policy Checklist.

Statistics

For all statistical analyses, confirm that the following items are present in the figure legend, table legend, main text, or Methods section.

n/a	Confirmed	
☐	☒	The exact sample size (*n*) for each experimental group/condition, given as a discrete number and unit of measurement
☐	☒	A statement on whether measurements were taken from distinct samples or whether the same sample was measured repeatedly
☐	☒	The statistical test(s) used AND whether they are one- or two-sided *Only common tests should be described solely by name; describe more complex techniques in the Methods section.*
☐	☒	A description of all covariates tested
☐	☒	A description of any assumptions or corrections, such as tests of normality and adjustment for multiple comparisons
☐	☒	A full description of the statistical parameters including central tendency (e.g. means) or other basic estimates (e.g. regression coefficient) AND variation (e.g. standard deviation) or associated estimates of uncertainty (e.g. confidence intervals)
☐	☒	For null hypothesis testing, the test statistic (e.g. *F*, *t*, *r*) with confidence intervals, effect sizes, degrees of freedom and *P* value noted *Give P values as exact values whenever suitable.*
☒	☐	For Bayesian analysis, information on the choice of priors and Markov chain Monte Carlo settings
☐	☒	For hierarchical and complex designs, identification of the appropriate level for tests and full reporting of outcomes
☐	☒	Estimates of effect sizes (e.g. Cohen's *d*, Pearson's *r*), indicating how they were calculated

Our web collection on statistics for biologists contains articles on many of the points above.

Software and code

Policy information about availability of computer code

Data collection | Data were collected using custom-built MATLAB 8.6 (R2015b) scripts with the open-source Psychtoolbox 3.0.14 software extension.

Data analysis | R (R Core Team, 2023) v.4.2.3. was used for all statistical analyses and data visualisations; MATLAB 8.6 (R2015b) and Fieldtrip (20230223) were used for data preprocessing procedures; Python v.3.10.6 was used for post preprocessing of iEEG data (i.e., calculation of aperiodic slopes); FreeSurfer software was used to estimate regional gray matter volumes. The following packages were used for data analysis: YASA v.0.6.3., label4MRI v1.2, tidyverse v.2.0.0, lme4 v.1.1.34, splines v.4.2.3, lmerTest v.3.1.3, car v.3.1.2., ggeffects v.1.3.2, ggplot2 v.3.4.4. All code for data analysis, including generation of figures, can be found at: https://tinyurl.com/m5yfc9ny.

For manuscripts utilizing custom algorithms or software that are central to the research but not yet described in published literature, software must be made available to editors and reviewers. We strongly encourage code deposition in a community repository (e.g. GitHub). See the Nature Portfolio guidelines for submitting code & software for further information.

Data

All manuscripts must include a data availability statement. This statement should provide the following information, where applicable:

- Accession codes, unique identifiers, or web links for publicly available datasets
- A description of any restrictions on data availability
- For clinical datasets or third party data, please ensure that the statement adheres to our policy

> Data used for analysis can be found at: https://tinyurl.com/m5yfc9ny.

Research involving human participants, their data, or biological material

Policy information about studies with human participants or human data. See also policy information about sex, gender (identity/presentation), and sexual orientation and race, ethnicity and racism.

Reporting on sex and gender	All subjects were neurosurgical patients undergoing iEEG monitoring for seizure management, and sex was determined retroactively based on hospital records. Demographic data including sex and age are provided on page 4 of the manuscript. Data from 63 male and 38 female patients were included in this study. No sex-based analyses were performed.
Reporting on race, ethnicity, or other socially relevant groupings	Information related to race and ethnicity were provided during the consent process and is available upon request.
Population characteristics	See above. Patients were aged 5 - 55 years.
Recruitment	Patients were recruited from Northwestern Memorial Hospital, the Ann & Robert H. Lurie Children's Hospital of Chicago, the Children's Hospital of Michigan, the University of California (UC), San Diego Rady Children's Hospital, UC Irvine Medical Center, UC Davis Medical Center, UC San Francisco Medical Center, Mount Sinai Hospital, California Pacific Medical Center, St. Louis Children's Hospital, and Nationwide Children's Hospital. The institutional review boards of Northwestern University (no. STU00215843), Lurie Children's Hospital (no. 2022-5020), Wayne State University (no. 048404MP2E), UC Irvine and UC San Diego (no. 2014-1522), UC Davis (no. 1623773-1), UC San Francisco (no. 10-03842), Mount Sinai (no. STUDY-22-00529), California Pacific Medical Center (no. 666687-17), Washington University in St. Louis (no. 201102222), and the Nationwide Children's Hospital (no. 2020N0022) approved the study in accordance with the Declaration of Helsinki. Written informed consent was obtained from participants aged 18 years and older and from the guardians of participants aged under 18 years. Written assent was obtained from participants aged 13 – 17 years and oral assent was obtained from younger children. The recruitment process may introduce self-selection bias, as patients who consented to participate may differ from those who declined. However, we recruited patients from hospitals across the Midwest, California, and New York to minimize bias. Additionally, the focus on academic medical centers could lead to clinical setting bias, where the severity of conditions or treatment histories differ from those in community hospitals.
Ethics oversight	All subjects provided written informed consent in accordance with the Declaration of Helsinki as part of the research protocol approved by the Institutional Review Board at each hospital.

Note that full information on the approval of the study protocol must also be provided in the manuscript.

Field-specific reporting

Please select the one below that is the best fit for your research. If you are not sure, read the appropriate sections before making your selection.

☒ Life sciences　　☐ Behavioural & social sciences　　☐ Ecological, evolutionary & environmental sciences

For a reference copy of the document with all sections, see nature.com/documents/nr-reporting-summary-flat.pdf

Life sciences study design

All studies must disclose on these points even when the disclosure is negative.

Sample size	The sample consisted of 101 patients aged 5-55 years who underwent iEEG monitoring as part of clinical management of seizures. Human iEEG research is limited by the availability of neurosurgical patients. From this perspective, the majority of iEEG work is based on relatively small sample sizes (e.g., n of 4-10) and cannot consider age-related or other sources of inter-individual variability (Johnson & Knight, 2023). Here, we analysed data from 101 individuals to enable sufficient statistical power to consider age-related variability. As such, this sample size is larger than most iEEG work, and far larger than any developmental iEEG study focussing on pre-defined regions of interest.
Data exclusions	Patients with major lesions, prior surgical resections, noted developmental delays, or neuropsychological memory test scores <80 were considered ineligible.
Replication	No replications were performed.

Randomization	All analyses were performed on the full sample. No randomization was performed.
Blinding	All data preprocessing routines and analyses of aperiodic electrodes were performed blinded to experimental condition and iEEG electrode placements.

Reporting for specific materials, systems and methods

We require information from authors about some types of materials, experimental systems and methods used in many studies. Here, indicate whether each material, system or method listed is relevant to your study. If you are not sure if a list item applies to your research, read the appropriate section before selecting a response.

Materials & experimental systems

n/a	Involved in the study
☒ ☐	Antibodies
☒ ☐	Eukaryotic cell lines
☒ ☐	Palaeontology and archaeology
☒ ☐	Animals and other organisms
☒ ☐	Clinical data
☒ ☐	Dual use research of concern
☒ ☐	Plants

Methods

n/a	Involved in the study
☒ ☐	ChIP-seq
☒ ☐	Flow cytometry
☒ ☐	MRI-based neuroimaging

Plants

Seed stocks	*Report on the source of all seed stocks or other plant material used. If applicable, state the seed stock centre and catalogue number. If plant specimens were collected from the field, describe the collection location, date and sampling procedures.*
Novel plant genotypes	*Describe the methods by which all novel plant genotypes were produced. This includes those generated by transgenic approaches, gene editing, chemical/radiation-based mutagenesis and hybridization. For transgenic lines, describe the transformation method, the number of independent lines analyzed and the generation upon which experiments were performed. For gene-edited lines, describe the editor used, the endogenous sequence targeted for editing, the targeting guide RNA sequence (if applicable) and how the editor was applied.*
Authentication	*Describe any authentication procedures for each seed stock used or novel genotype generated. Describe any experiments used to assess the effect of a mutation and, where applicable, how potential secondary effects (e.g. second site T-DNA insertions, mosiacism, off-target gene editing) were examined.*